Fibration symmetry uncovers minimal regulatory networks for logical computation in bacteria

Luis A. Álvarez-García

Levich Institute and Physics Department, City College of New York, New York,
NY 10031, USA

Wolfram Liebermeister

Université Paris-Saclay, INRAE, MaIAGE, 78350 Jouy-en-Josas, France

Ian Leifer

Levich Institute and Physics Department, City College of New York, New York,
NY 10031, USA

Hernán A. Makse*

Levich Institute and Physics Department, City College of New York, New York,
NY 10031, USA

October 18, 2023

Abstract

Symmetry principles have proven important in physics, deep learning and geometry, allowing for the reduction of complicated systems to simpler, more comprehensible models that preserve the system's features of interest. Biological systems often show a high level of complexity and consist of a high number of interacting parts. Using symmetry fibrations, the relevant symmetries for biological 'message-passing' networks, we reduced the gene regulatory networks of *E. coli* and *B. subtilis* bacteria in a way that preserves information flow and highlights the computational capabilities of the network. Nodes that share isomorphic input trees are grouped into equivalence classes called fibers, whereby genes that receive signals with the same 'history' belong to one fiber and synchronize. We further reduce the networks to its computational core by removing "dangling ends" via k-core decomposition. The computational core of the network consists of a few strongly connected components in which signals can cycle while signals are transmitted between these "information vortices" in a linear feed-forward manner. These components are in charge of decision making in the bacterial cell by employing a series of genetic toggle-switch circuits that store memory, and oscillator circuits. These circuits act as the central computation machine of the network, whose output signals then spread to the rest of the network.

Significance Statement

Biological systems often are constituted by complex interactions between a big number of different components, as such, being able to reduce their complexity in order to understand their behaviour is of paramount

---

*Corresponding Author: hmakse@ccny.cuny.edu

1

importance. We use symmetry principles, in a manner akin to physics, to reduce the Transcriptional Regulatroy Networks of *E. coli* and *B. subtilis* to reveal the computational structure at the core of these networks responsible for driving their dynamics. The computational core of this networks is embedded with gene logical circuits, such as toggle-switches and oscillatory circuits, which ultimately are in charge of the decision making in the bacterial cell.

1   Introduction

1.1   Complexity reduction via symmetries

A main feature of biological systems is their inherent complexity, reflected in the sheer mass of quantitative parameters and details needed to describe the system precisely [36]. High-dimensional parameter spaces are ubiquitous in biological systems. The human brain, an evident example, consists of ~ 80 billion neurons with intricate connections between them. In the mouse brain, with three order of magnitude less neurons, difficult techniques need to be employed to understand the collective macroscopic behaviour [47, 48]. Even in the *C. elegans* neural system, composed of merely 302 neurons, it is not known how this tiny connectome leads to function, and low-dimensional models are needed and regularly used [71]Finding low-dimensional effective models to describe the dynamics of these systems is crucial to understand how function and collective behavior emerge from the complex dynamics of the system's constitutive elements.

In physical systems, one is also confronted with high-dimensional models to fit experimental data. However, well defined theoretical methods have been developed that use the symmetries of the system to reduce the model to a more comprehensible description that preserves the relevant attributes to be studied. Indeed, symmetry principles are physicists' basic arsenal to confront systems with high complexity, ever since Emmy Noether's seminal theorem, showing that the symmetries of the Lagrangian lead to global conserved quantities, e.g. translational/rotational symmetries leading to linear/angular momentum conservation, or time invariance leading to energy conservation. Knowing the system's symmetries, we can therefore simplify the system while preserving its properties, and still observe the same physical results, hence allowing us to work with simpler global quantities (momentum, energy) that preserve the relevant traits to be investigated. This idea led to the application of symmetries across all branches of physics, from relativity, to quantum mechanics and culminating in the standard model of physics that explains within a unified gauge symmetry group U(1)$\times$ SU(2)$\times$SU(3) all elementary particles and interactions, with the only exception of gravity so far.

Scale-invariance is another ubiquitous symmetry in the natural world allowing for simpler descriptions of physical systems with no free parameters. And this idea has been applied to everything from critical phase transitions of matter [38] to flocks of birds [7, 13]. In statistical physics, critical phenomena describe critical systems (liquid-gas transition, superconductivity, superfluidity, phases, etc) in a universal way since the microscopic details of the particle interactions are washed out by the large fluctuations at the critical point. In these systems, renormalization group theory is used to 'smooth out' details of the system to focus on the effective 'larger-picture' models that arise at criticality. Landau theory and spontaneous symmetry breaking then provided an explanation for the existence of phases of matter and the emergence of universal critical behavior unifying condensed matter and high-energy physics.

1.2   Symmetries in geometry and machine learning

However, the approach of simplifying and ultimately understanding a system through its symmetries did not originate from physics. Indeed, we are all familiar with the shapes of a square and a sphere: symmetries are synonymous with shape and geometry. In 1872, the very influential *Erlangen Programme* proposed by Felix Klein[35] sought out to unify the disperse and apparently different geometries sprawling from 19th century mathematics, from Euclidean to non-Euclidean (affine, elliptic, hyperbolic, Riemannian). The unification was achieved under the guise that different geometries were concerned with the study of symmetry under different transformations that preserve some properties of the studied objects. For example Euclidean geometry studies rotations and translations which preserve length and angles, affine geometry is concerned with affine transformations that preserve parallelism, etc. At the time of Klein, the theory of symmetry groups had been introduced by Galois for the study of solutions of algebraic equations (concerning with symmetries in the roots of polynomials). Klein then proposed that the same symmetry groups were the fundamental organizing

principle to unify all geometries. Klein's program has had the most profound influence in the 'geometrization' of physics from Einstein's theory of general relativity to the standard model.

Continuing to nowadays, symmetries and geometry are fundamental tools in data science and machine learning. Machine learning seeks a dimensional reduction of high-dimensional data to a low-dimensional representation, and symmetries have been largely exploited in this endeavor [11]. Other machine learning techniques to reduce the dimensionality of data are principal component analysis [6], clustering methods, renormalization group [47, 48], sloppy models [69] and others [62, 60, 61].

In machine learning, symmetries are transformations applied to data that, while changing the numerical representation of the data, do not change the underlying object that the neural network is learning. For example, translating or rotating an image of a cat should not change the classification of the image as a cat. Likewise, permuting the labels of a graph or rotating a molecule in three dimensions should not change their classification. In turn, symmetries within the data structure can be used to develop a neural network that respects the same symmetry. A typical example is translational invariance which is built in in convolutional neural networks or graph neural networks invariant under permutations. Ultimately, symmetry can be thought of as a general unifying blueprint for the most popular architectures spanning from convolutional neural networks, recurrent neural networks, graph neural networks to transformers [11]. Following the Erlangen Programme, the symmetrization of deep neural networks is called Geometric Deep Learning [11].

1.3 Geometric Biology

Inspired by the progress in the application of symmetries and geometry in all these areas, here we ask if the same geometrization can be invoked to tame biological complexity, and if so, then precisely how. We will see below that the answer is yes, but with a caveat; the symmetries of physics and deep learning cannot be directly applied to biology.

In physics and deep learning, geometrization is performed through the use of group symmetries. These symmetries are called automorphisms and form the symmetry group of either the physical system or the high-dimensional data learned by machines. These groups satisfy the four axioms of group theory: composition, inverse, identity and associativity. Applied to graphs, automorphisms preserve the adjacency of nodes.

However, we have found before [52, 53, 39, 40] that automorphisms are too restrictive to be applicable in biological networked systems. Indeed, nobody has ever found evidence that the automorphisms can be applied to biological systems. It seems that the symmetries that were so successful in physics, deep learning and geometry cannot be translated to biochemical systems, even though biology emerges from physics (through chemistry).

This conundrum was solved by the discovery that symmetries still emerge in biology, but of a different kind. The symmetries of living networks are a more relaxed form, calling instead for the use of groupoids (transformations that satisfy associativity, inverse and identity but not composition) rather than groups [64, 23], and putting forth the concept of fibration symmetries. These symmetries are based on graph fibrations [9], which in turn are a particular case of Grothendieck fibrations from category theory [25]. Fibration symmetries are generalizations of automorphisms (every automorphism is a fibration but not the opposite) that impose less strict conditions on the structure of the networks, compared to automorphisms. They are graph symmetries of the input trees and do not need to preserve the full adjacency of nodes, thus allowing the emergence of the enormous complexity of the biological world as compared with physics.

1.4 Fibration symmetry

For a network automorphism, you require the full adjacency matrix of the network to be preserved by the transformation. This means that for any single node both its input degree and its output degree must be preserved to its automorphic, or symmetric, graph. The problem is that this appears to be too much of a restrictive condition for real biological networked systems. As discussed, real biological networks tend to have a big number of component nodes, from *E. coli*'s 1843 genes in its TRN, to the human brain's multiple billion neuron. If two nodes with similar connectivity have just one single edge of a difference, this ruins the whole automorphic structure for the network.

If we stop requiring for the output degrees to be preserved, this less restrictive conditions now exhibit a plethora of different symmetric structures[52, 40, 39]. The need to drop this constraint is what makes

it necessary to work with the groupoids formalism instead of groups. A consequence of this relaxation in constraints, is that we are now actually only looking at the inputs of the nodes. It is by looking the symmetries in the input histories of nodes that these symmetries, fibration symmetries, are found on networks. The input history of a node corresponds to its *input tree*, the rooted tree at the node in question that includes all the incoming pathways to the node. Two nodes with the same input trees receive the exact same information, this makes them redundant as information pathways for the network.

Furthermore, since the output of nodes depend, ideally, only on its inputs this implies symmetric nodes with identical input trees have in fact the same output, in other words symmetric nodes become synchronous. This is of importance given that the phenomena of gene co-expression and synchronization is known to be of importance for the cell's overall functioning and energetic efficiency considerations. Indeed, cluster synchronization has been observed in a range of biological situations [7, 48].

Fibration symmetries are then symmetries of the information pathways where the signals, or messages, are being sent. This symmetries are found by identifying sets of nodes with identical input trees, or fibers. This then becomes very useful since it allows for a reduction of the network by collapsing symmetric nodes without compromising the information flow of the network. This will be of tremendous importance to understand the structure of the TRNs of bacteria by allowing us to reduce the complexity of this networks without affecting the information flow of the full network.

1.5 Transcriptional Regulatory Networks

Below we focus on the case of bacterial gene regulation, exemplifying complex signal processing in biology. To describe the dynamics in a Transcriptional Regulatory Network (TRN) by ODEs, we need a large number of microscopic parameters describing the gene input functions. The model bacterium *E. coli* possesses a genome of more than 4000 genes, of which 1843 are known to have regulatory functions in the transcriptional network (see [52] and its SI, as of RegulonDB's aggregate of results to date [68]). Every transcriptional interaction between two genes (edges in the network) requires multiple parameters for a precise mathematical description of the genes' expression dynamics [36]. These effective parameters capture the gene regulatory process from transcription, translation, protein folding, to mRNA and protein degradation, including details like binding and unbinding to DNA, ribosome and polymerase binding, mRNA and protein life-times, etc [36].

While most of these parameters are unknown, structural analyses of the network have led to considerable insights. Previous studies focusing on the topology of *E. coli's* GRN have searched for structures on the smaller and larger scale. They identified building blocks by statistical over-representation in the network, as compared to randomized networks [59, 49], the so-called network motifs. This proved that the network structure most likely is a results of evolutionary pressures rather than a randomly connected network, as expected. Even though the individual dynamics of some network motifs is more or less understood [59, 49], given that they are in essence local structures they do little to unravel the global topology of these networks or the global dynamics. Also, statistical significance alone is not synonymous with biological relevance (a car is full of bolts, yet irrelevant to explain its functioning).

On the large scale, it has been proposed that the network is feed-forward [42, 45, 16, 59], where signals flow unidirectionally from a core of sensors or master regulator genes through a series of parallel layers down to an outer periphery in feed-forward manner [16, 59, 49]. But there are also feedback loops in the system which further complicate this picture. So what is the relevant structure at the 'center' of these systems, the core structure in charge of decision making, which genes belong to it, and how does this structure control the rest of the network?

1.6 Complexity reduction through fibrations: constructing a minimal TRN

In this paper, we describe how to reduce the complexity of TRNs to their "minimal computational core" by applying the concept of graph fibrations [15, 9]. We have shown before [52] that this is the proper symmetry that allows for a reduction of *E. coli's* TRN to a more understandable structure by allowing a breakdown of the network into its building blocks. Our symmetry notion exploits the symmetries in the input history each node, or gene, receives. Based on these notion of symmetry we present a novel method to reduce any directed *'message-passing'* network, with a flow of signals between nodes, to what we call its computational core.
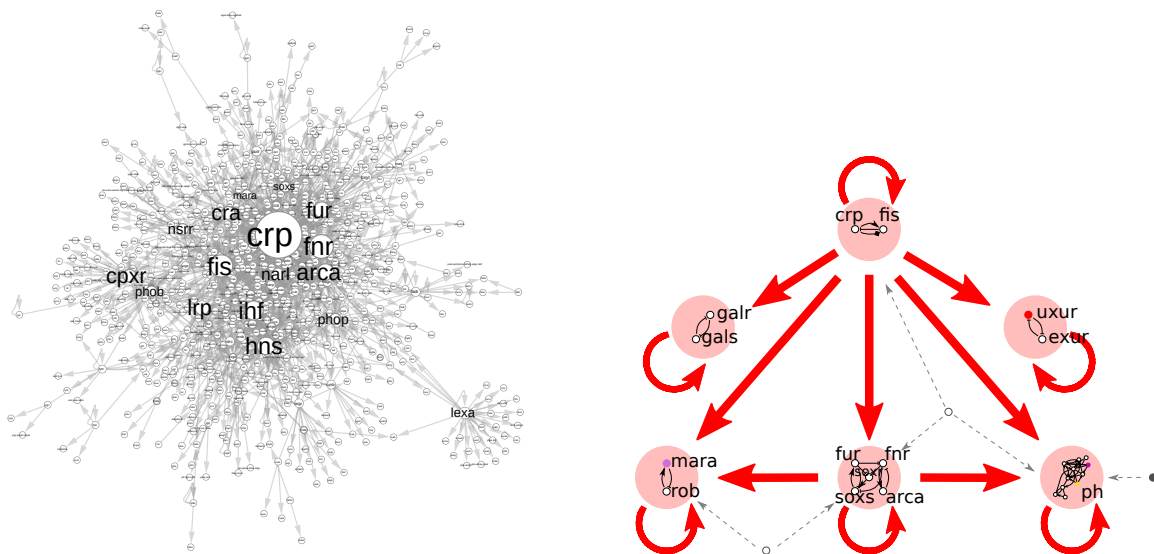
Figure 1: Main results on *E. coli*'s TRN. On the right, we show the weakly connected component (i.e. small disconnected pieces of the network are not shown, since they don't play a significant role for the network's dynamics) of the full 879 nodes operon-TRN for *E. coli*, size of the nodes and font size are proportional to out-degree of the node. Right: we show a representative sketch of the core of the TRN left after application of our reduction method, simply illustrating the signal flow between its different components (bigger red nodes), the strongly connected components (SCCs) of the network: components of the network where every node can be reached from every other node. Smaller nodes represent the genes present at the "computational core" of the network, colored nodes represent collapsed-fiber nodes. The red arrows represent multiple edges between the components. The nodes outside the components are examples of controller nodes, of 1st, 2nd and 3rd type, which send signals to different components. Interestingly, two feed-forward structures exist between the components: the central *crp-fis* SCC regulates the *soxS* SCC and both regulate jointly, in one feed-forward structures the ph SCC, and in the other the *mara-rob* SCC. Considering only the larger red nodes and arrows gives the condensation of the core, the acyclic SCC-quotient network.

Symmetries supplemented by graph theoretical tools are applied to reduce the complexity of TRN to its minimal structure as sketched in Fig. 1 and shown with more detail in Fig. 7. After the reduction of the TRN to its minimal structure, this minimal structure is then analyzed in three more steps. The overall procedure consists of five steps:

- Step 1. Collapsing: graph reduction via symmetry fibrations, by collapsing all the redundant symmetric pathways. This represents a reduction of 70% in *E. coli*'s TRN.

- Step 2. Pruning: reduction via k-core decomposition (inverse injective fibration), this steps removes nodes like enzymes that do not regulate other genes directly. This represents a reduction to only 2% of the original *E. coli*'s TRN.

- Step 3. Decomposition of the Minimal TRN: breaking down the core minimal network by strongly connected components (SCC).

- Step 4. Computational core: Identification of symmetry breaking building blocks in the Minimal TRN.

- Step 5. Simple cycles: Identification of simple cycles in the Minimal TRN's SCCs.

Step (1) and (4) decompose the genetic network into its building blocks by using fibration symmetries and broken symmetries, respectively. Together, these steps lead to the identification of the function for every single gene in the Minimal TRN as belonging to three general classes of genes:

- (1) A set of synchronized symmetric fibers

- (2) Regulators of the SCCs

- (3) Broken fibration symmetry circuits within the SCCs, which can be further classified into:

  - (3.1) memory devices(flip-flops or toggle switches): broken symmetries of the $n = 2$ fiber
  - (3.2) oscillators.

The fibers are assembled from five basic fibration building blocks, Fig. 2:

- (1) Trivial fibers made of regulons, operons, etc., with no self-loops within the fibers. Hence we call them $n = 0$, and are fully feed-forward. They make up 67% of the building blocks in *E. coli*.

- (2) Feed-forward fibers (FFF), where there is self-loop present in the fiber. They make up 26.4% of *E. coli*'s building blocks. They are subdivided in sub-classes of:

  - (2.1) 0-FFF, 14%,
  - (2.2) 1-FFF, 9%,
  - (2.3) 2-FFF, 3%.

- (3) Fibonacci fibers φ-FF with fractal dimensions $\varphi = 1.61, 1.31$, and 1.15 of loops (3.3%). These occur when the fibers also send back signals to the regulators.

- (4) $n = 2$ fiber (2.2%). The $n = 2$ symmetry is further broken to form the memory and oscillatory units composing the SCCs.

- (5) Composite fibers: a composition made of the previous ones (1.1%).

We find that these building blocks are arranged in a large-scale structure that contrast with previous representations of the bacteria TRN.

1.7   The TRN as a decision-making computer

A main feature of TRNs, which we emphasize here, is that signals do not only propagate in "forward direction" between different layers, but can also cycle like in feedback loops. Network structures that only allow forward transmission map input to output signals of similar shapes, possibly blurred, inverted, or time-delayed. They may also aggregate several inputs and general several outputs, but they do not have memory. Circuits in which signals can cycle show more complex behavior: they can stabilize an output variable, generate oscillations, and may internally store information, like a flip-flop in electronics or toggle-switch in synthetic biology.

In electronics, feed-forward circuits are called "combinatoric logic circuits" and are memoryless digital circuits whose output at a given time depends only on the combination of its inputs. These circuits are made of standard logic gates like NOR and NAND. On the other hand, circuits with feedback are called "sequential logic circuits". Their outputs depend on both their present inputs and also their previous output state. This feedback loop provides them with memory, since the circuit is able to remember its state even when the external input is removed. Their building blocks are electronic flip-flop circuits which are analogous to biological toggle switches. Combinatorial and sequential circuits are the "decision making" machinery behind the logical function of the electronic circuit. They are also needed in the cell, if the cell is to perform as a computational biological machine.

We find that in the TRN, these two modes of signal transmission appear both on small and on large scale. On the small scale of single nodes, there are local circuits that only rely on forward transmission and others that contain feedbacks. These feedback circuits are the $n = 2$ fibers and their broken symmetries forming oscillators and toggle-switches, seen on figure 2. On a large-scale level, the TRN consists of strongly connected components in which signals can cycle on "information vortices", while the vortices, between each other, are connected in a "forward signaling" manner (Fig. 1).
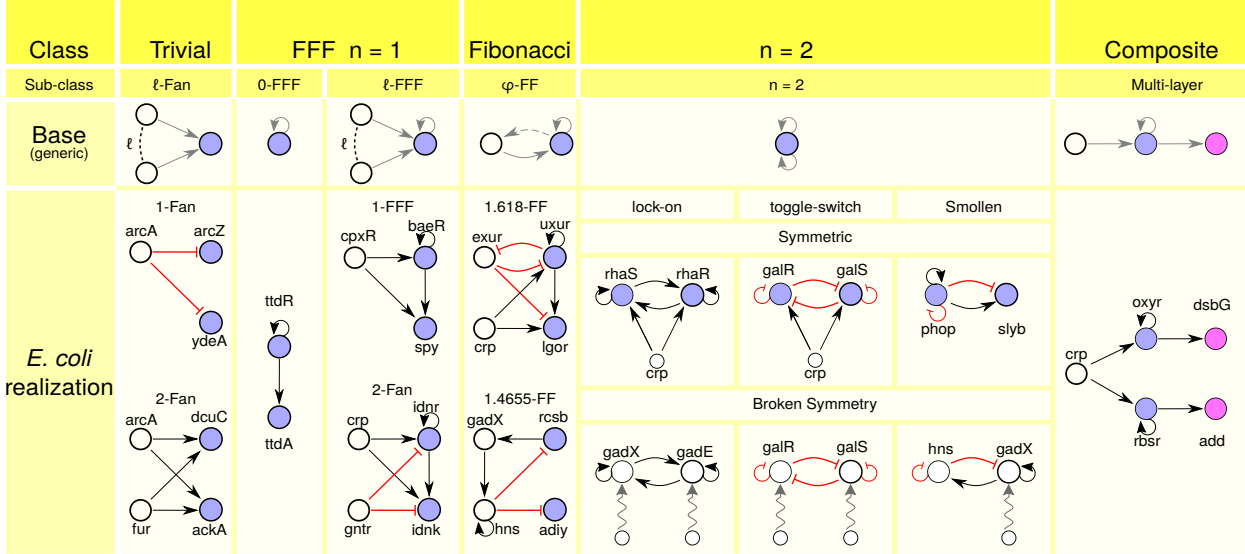
Figure 2: Basic gene circuit building blocks in the Gene Regulatory Networks of *E. coli* and *B. subtilis*. The networks can be seen as assemblies of 5 basic fibration building blocks: (i) trivial fibers. An ℓ number of external regulators identically regulate the genes in a fiber, making them synchronous. Operons with only one promoter correspond to a building block analogous to this, where the colored nodes represent the genes belonging to the operon (perhaps with more colored nodes in the fibers, depending on the number of genes in the operon). (ii) The feed-forward fiber and within it, its sub-classes of ℓ-FFF with ℓ external regulators . The FFF fiber is defined by a feed-forward motif with a self-loop in the synchronous set of genes, and the number of ℓ external regulators. (iii) The Fibonacci fiber, φ-FF. A more complex building block, defined by a fractal dimension branching ratio that occurs given the presence of a self-loop and a feed-back regulation back to the regulator(s) from the fiber. The observed Fibonacci fibers in *E. coli* have a branching ration between 1 and 2, placing this building block in between the FFF fibers and the n=2 fibers. (iv) the n=2 fibers, defined by two self-loops in the synchronized genes. When this symmetry is broken it forms the memory and oscillatory units embedded in the SCCs. And finally (v) composite fibers of the previous ones. By adding different types of the previous 4 building blocks, in a sequential manner, a composite fiber is obtained. An interesting consequence of this is the synchronization of genes that may be far apart from each other and don't share any regulation.

1.8 The TRNs of two model bacteria: Large-scale components and small-scale circuits

For the TRNs of *E. coli* and *B. subtilis*, two main bacterial model organisms, we found that the structure in charge of decision making corresponds to just 42 genes for *E. coli* and 22 for *B. subtilis*.

The TRN of *E. coli*, shown in Fig. 1b, comprises three major SCCs: one for carbon utilization and two for stress and PH regulation (there are two extra two-genes SCCs that only receive information from the carbon SCC). These SCC exchange feed-forward signals between each other and receive external inputs from the small number of controller genes. Internally, they are made of symmetry-broken memory-storing toggle-switches and oscillators; the two primary components of any computer. Thus, the TRN can be seen as a computational machine where the memory is stored and controlled by broken symmetry circuits within the 3 major SCCs. The flip-flops in the SCCs control the turning on and off of a set of symmetric fibers representing clusters of genes displaying coherent synchronization in gene co-expression.

These synchronous fibers transmit the "information" to other parts of the cellular network, such as the metabolism. In turn, a set of controller genes (regulatory genes participating in one-, two- or three-regulations of SCCs) control the SCCs by switching the flip-flops into their different binary bistable states (ie, zeros and ones). Thus, the SCCs act as the decision-making units turning on and off the states of the fibers

under their control.

The minimal TRN network has vortices on a large scale, and feed-forward and feedback circuits on a small scale. Recognizing this structure help us understand what the network can do and what are the functions of different parts of the network. Hence, we not only reduce the TRN to its core computational structure (by omitting symmetric and peripheral nodes), but also we identify the "information vortices" and the local gene circuits that process signals and store information, and are therefore capable of calculations, comparable to a silicon-based computer. Our results show that bacterial TRNs have exactly this structure.

The system of SCCs represents the smallest computational subunits which cannot be reduced further neither by the fibration symmetries nor by smaller strongly connected components. Thus, this structure represents the "minimal TRN" structure of the cell. The central subunit of this minimal TRN is the carbon SCC which transfers information downstream to the other two main SCC components for ph and stress regulation. These two SCCs are further connected one way, forming a feed-forward loop representing the core of the genetic computing system, thus capturing the minimal TRN that cannot be reduced further. Within these three major connected components, the information travels along cycles turning on and off the toggle switches that store the memory in their states.

1.9   Evolutionary origin of fibration symmetries

Mathematically, fibrations are built by the lifting property; a mechanism that can be mapped to the duplication of genes and edges in the biological graph. This suggests that the emergence of fibration symmetry in the TRN is a major design principle of the genetic network consistent with its dynamical evolution as fibrations are created.

This evolutionary design principle of the TRN follows the lifting of genes and edges from a primordial set of fibration bases depicted in Fig 1. The bases of the building blocks form symmetric fibers by duplication and memory storage circuits, and oscillators by breaking the symmetry of the symmetric fibers. This lifting-driven dynamical evolution creates the core of the computational decision-making of the cell that represents the assembly of the genetic collective intelligent device.

2   Methods

2.1   Transcriptional Regulatory Networks (TRNs)

Gene expression in cells is regulated in response to the cells' environment and internal state. In bacteria, gene expression is governed by various global mechanisms (e.g. via sigma factors, varying activity of the global transcription and translation machinery), and also "regional effects" on the chromosome correlated expression or nearby genes on the chromosome), play a role. Here we disregard these effects and focus instead on regulation by specific transcription factors (TFs), whose activities depend on their own expression levels and can be modulated by small-molecule binding. Transcription factors bind to DNA sites called promoters that regulate specific genes. They can activate or repress the transcription of genes, thus increasing or decreasing the expression levels of their target genes. Metabolites can bind to different TFs and modify their regulations, and thus modulate the expression levels of their genes. The metabolites may come from the outside environment of the cell or may be products of the metabolism of the cell itself, providing a feedback mechanism in which the metabolic state of the cell informs the regulation of transcription [36, 1, 45].

The Transcriptional Regulatory Network (TRN) represents the direct regulatory effects between Transcription Factors (TFs). TFs themselves are proteins coded from genes, this means a gene codes for a TF that binds to another gene's promoter region and regulates its expression. In the network, this is considered a directed link between the first and the second gene. The type of edge corresponds to the type of regulation being performed by the transcription factor, being activation, inhibition or dual (depending on how the TF binds to the promoter region). Together, all such regulations form the TRN, which determines the expression of individual genes according to the cell's sensed environment and its own internal, for instance metabolic, states. Gene regulation processes external signals to compute and enact future expression levels. This process of sending regulatory messages as signals across genes defines the information flow in the gene network. The signal can be though of as an 'information package' or 'message passing' being sent from the source gene to the target gene.

In this paper we consider only the transcriptional regulation between genes, other forms of regulation including signaling and metabolic pathways also display symmetries. Their symmetries and structures will be treated in subsequent papers.

2.2 Gene regulation dynamics

Gene expression dynamics in the TRN can be modeled using ordinary differential equations (ODEs) [20, 1] for mRNA and protein concentrations, assuming known gene regulatory functions [8]. While we will not model signal transmission dynamics, it is necessary to understand how a network of regulatory arrows can be translated into a dynamical system and vice-versa. This clarifies both the importance of network structure and the importance of other, quantitative and gene-specific details that are not represented by network structure alone. In a simple possible model, each gene is described by a single dimensionless expression value, representing the protein concentration, that is, the gene product. For a protein concentration x_i expressed by gene i regulated by a set of genes j expressing transcription factors with activity concentration given by y_j, the expression dynamics can be modeled by the following lumped ODE:

$$\frac{dx_i(t)}{dt} = -\alpha x_i + F[\gamma_j f_K(y_j)], \tag{1}$$

where $x_i(t)$ is the time-dependent protein concentration expressed by gene i, α corresponds to its degradation constant (including the often dominating effect of dilution), γ_j is the maximal synthesis rate of the protein product and $f_k(y_j)$ is the interaction or input function between the TF y_j and the binding site of gene i which depends on the dissociation constant K between them.

The coupling term $f_K(y_j)$ for an individual TF y_j interaction is usually modeled as a sigmoid function such as a Hill function [20, 1], or a Heaviside step function, its Boolean logic approximation [39, 55]. Qualitatively, the Heaviside step function can be thought of as a Boolean logic function in the following intuitive manner [55]: each gene can take the "on" or "off" state, an activation signal being a proxy for *"turning on"* the gene while an inhibition signal is a proxy for *"turning off"* the gene.

The function $F[\cdot]$ combines the regulatory input functions from all inputs y_j of the gene i. They have been proposed and measured [58, 31]. Some input functions can be taken as logical AND with $F[\cdot]$ being a multiplicative function of its individual gene inputs, or OR gates with $F[\cdot]$ being additive on the inputs [46]. Other input functions can be more complicated forms involving many-body interactions where three or more inputs interact in a common way. These interactions are treated by hypergraphs, not by graphs. In this paper we consider only two-body interactions captured by a graph. We leave the study of hypergraphs for a follow up study, yet these considerations do not affect the general conclusions about the symmetries of the TRNs.

Equation (1) contains huge simplifications, given that in actuality one would need to known the precise values for the bindings of RNA polymerase, repressors, ribosomes, as well as transcript elongation and termination, just to mention a few, to do a more exact model. The parameters presented are lumped parameters to account for these phenomena in an effective manner [20]. Furthermore, in order to do a precise prediction for the entire TRN one would need to know these parameters for every edge of the network, in our case for our *E. coli*'s TRN-operon network there are 1,835 edges for example. It would be pretty much impossible to model this in an exact manner currently. What we do instead is to take the most drastic approximation and take the parameters to be the same for every edge. Later we will show that this approximation can be relaxed to same edge parameters for the outputs of each gene but different for different genes, unless that they do not participate in a multilayer fiber.

For the second step of the reduction process, discussed further in text, this is not very relevant since we are only interested in the out-ward flow of signals. This approximation allows us to do a huge improvement in understanding the structure of the network; as will be shown, it will reveal the ideal structure via symmetries from which small corrections due to the heterogeneous parameter space can be studied later on. The question is whether the admissible set of equations may break these symmetries or not. Our contention is that the heterogeneous parameters preserve the structure already imposed by the graph symmetries, and this is supported by the experimental evidence of gene synchronization (co-expression patterns) widely obtained for these systems.

2.3 Graph fibrations

The network reduction method explored in this paper is based on graph fibrations. Fibrations were introduced by Grothendieck [25] in the context of category theory and algebraic geometry. While the original work applies to fibrations between categories and could be a bit obscure for pedestrians, fortunately, categorical fibrations have been adapted to graph fibrations by Boldi and Vigna [9] in computer science. Their inspiration was a distributed system of processors needs to be synchronized in a coherent manner for proper global updates, as there is no point to have a processor waiting for its update out of sync from the rest. A computer system seen as a graph of processors with fibration symmetries then guarantees coherent optimal processing. As stated in the illuminating words in Vigna's blog on fibrations https://vigna.di.unimi.it/fibrations:

"If a graph G is used to represent the structure of a network exchanging messages, and the processors of the network execute the same algorithm starting from the same initial state, the existence of a fibration $\varphi : G \to H$ implies that, whatever algorithm is used, there are executions in which the behaviour of the nodes in G is fibrewise constant (i.e., all processors in the same fibre are always in the same state)."

This idea can be directly translated to the cell's TRN if we were to ever find that it functions as a computer, and it was enough inspiration to us to search for fibrations in the TRN [52].

We note that the condition that every processor executes the same algorithm is translated to the TRN as the condition that every input function has the same parameters. This condition is natural for computer processors but controversial for biology. Still, as usually done by physicists (remember the metaphor of the spherical cow, the legend of Gordian knot and Occam's razor), we translate this simplification to biology, and we deal with the consequences later.

A (directed) *graph* $G = (N, E)$ is a pair of nodes N and edges E, where each edge $e \in E$ is an unordered (ordered) pair of nodes, i.e. $e = (i, j)$ for $i, j \in N$ [27]. It is customary to define two functions $s, t : E \to N$ that map each the edge to its respective source and target nodes: $s(e) = s(i, j) = i$ and $t(e) = t(i, j) = j$.

A directed graph is strongly connected if there is a path between all pairs of vertices. *Strongly connected components* (SCC) of a directed graph are maximal induced subgraphs that are strongly connected.

A *graph morphism* $\varphi : G \to B$ is a mapping between two graphs $G = (N_G, E_G)$ and $B = (N_B, E_B)$ given by two functions $\varphi_N : N_G \to N_B$ and $\varphi_E : E_G \to E_B$ that satisfy

$$s_B(\varphi_E(e)) = \varphi_N(s_G(e)), \tag{2}$$

and

$$t_B(\varphi_E(e)) = \varphi_N(t_G(e)) \tag{3}$$

for every edge $e \in N_G$ [27]. Simply speaking, if any two nodes are connected in G, they are connected in B. This gives a type of commutative relationship, in which edges are mapped in such way that the image of the edge connects the image of the source to the image of the target, preserving the incidence relation between the source node and target node to their respective images.

A *graph fibration* is a graph morphism $\varphi : G \to B$ (between a graph G called the total space and a graph B called the base) in which for every node i in G, and every edge e' in B targeting its image ($i' = \varphi(i) = t(e')$), there is a *unique* edge $e \in E_G$ targeting i ($i = t(e)$) whose image is $e' = \varphi(e)$. That is, every edge targeting i' can be *uniquely* lifted to an edge in G targeting i. This condition is called the lifting property [9]. Consequently, multiple edges targeting a same node, in G, can not be collapsed to fewer edges in B, neither can new edges targeting the image of a node be added. Crucially though, nodes *can* be collapsed, if they possess isomorphic *input trees* implying synchrony, which will be defined in a moment.

The definition of graph fibrations is exemplified in Fig. 3A. The mapping to graph G_1 is clearly a morphism, since the images of all the nodes in G_1 are connected only when corresponding nodes in G are connected. Furthermore, this mapping is a surjective fibration since nodes 2 and 3 are collapsed with the map satisfying the lifting property.

The example mapping to graph G_2, is again a valid fibration. Indeed, it is easy to see that the original graph is embedded in G_2 making this map a morphism. Moreover, no new edges target any of the nodes of the original graph, hence the lifting property is satisfied. The mapping from graph G to graph G_3 does not correspond to a fibration because edges a' and c' can not be uniquely lifted at $\varphi(2)$, since they need to be lifted to a, f and c, g for the mapping to be a morphism. In practical terms, since the input from node 4 is lost, graph G_3 represents an entirely different dynamical system from graph G. If the graph G represents a TRN, genes $2'$ and $3'$ would have a different expression pattern than genes 2 and 3.
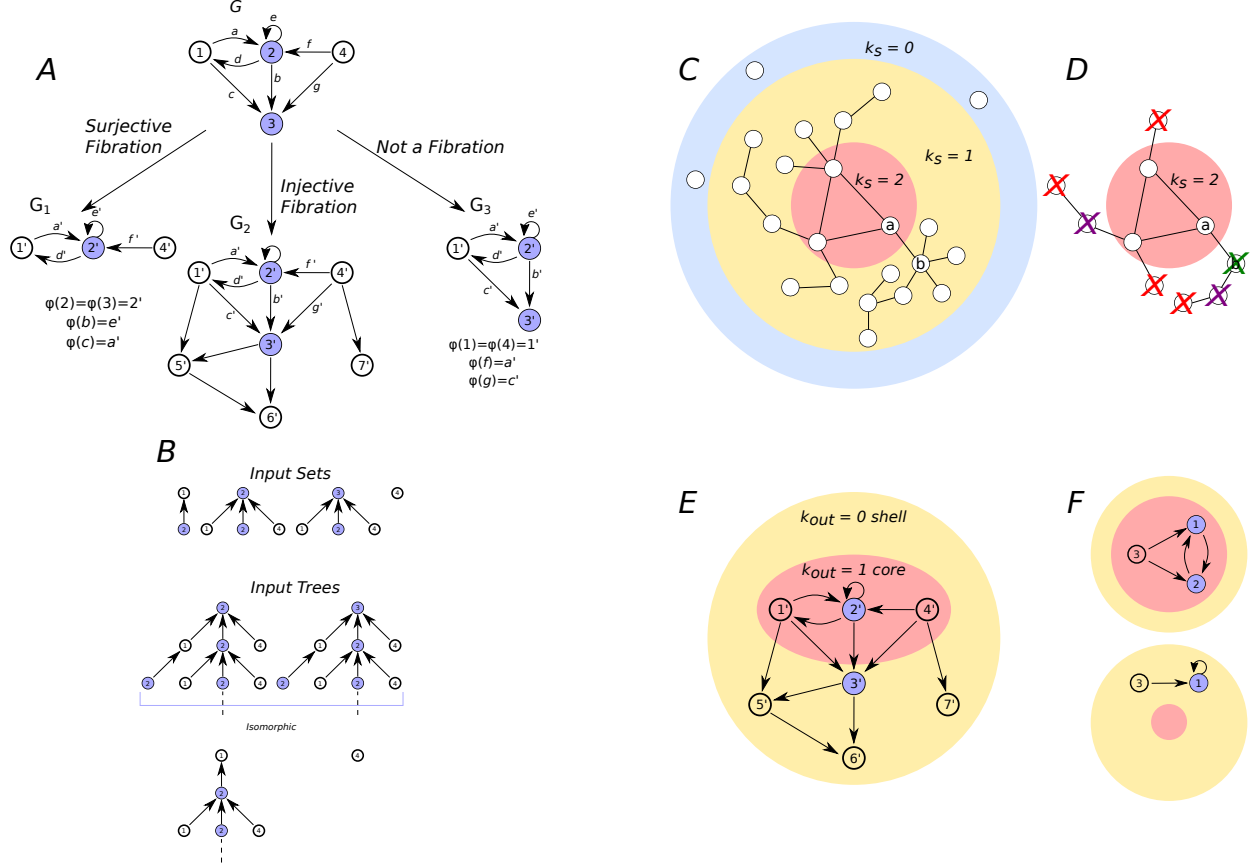
Figure 3: Fibration and k-core decomposition. **A** Graph G, a subgraph of the TRN of *E. coli*, shows a Fibonacci building block with class number $|\varphi_d = 1.6180, \ell = 2\rangle$ [52, 40]. The mapping from graph G to graph G_1, in the left, corresponds to a surjective fibration: all nodes with isomorphic input trees are collapsed to one (nodes 2 and 3 collapsed to 2'), all input trees are preserved. Mapping from graph G to graph G_2 is an injective fibration: all input trees are preserved and there are extra nodes included. The map from the graph G to graph G_3, which maps node 4 to 1' does not correspond to a fibration given that the input-tree of 4 (seen on **B**) is not preserved in its image node 1' in graph G_3, the same problem occurs with the images of nodes 2 and 3 (2' and 3' respectively), their input tree (seen on **B**) is not preserved as the former input from node 4 is no longer present in graph G_3. **B** Shows the input sets and input trees of nodes in graph G. **C** Schematic drawing of the k-core decomposition of an undirected network. Even though node b has a higher degree than node a, it is connected to nodes with smaller degree and has therefore a smaller coreness than node a. **D** Example of how to obtain the $k = 2$ core of the network in **C**. First, the nodes with degree less than 2 are removed. The remaining nodes are the ones shown, successive iterations remove the nodes crossed with colored X. Different colors stand for successive iterations: red is the first iteration, the second one is purple and the last one is green. **E** Example of the k-core decomposition of graph C from **A**. Even though node 5' on the outer $k_{\text{out}} = 0$ shell (in red) does have one output, once nodes 6' and 7' in the shell are removed, it will then be left with no output and will be removed as well. All the remaining nodes in the $k_{\text{out}} = 1$ core have at least 1 output after doing this process. **F** The bottom network corresponds to the symmetry fibration of the network on top. The SCC of nodes 1 and 2 is also fiber, after collapsing the fiber the SCC is lost and so the collapsed network becomes an acyclic graph, so it does not have a $k_{\text{out}} = 1$ core.

The notion of fibrations can be extended to graphs with various types of edges, such as a gene regulatory network which has edges corresponding to three types of interaction: activation, inhibition and dual (can act as either activation or inhibition). The concept of fibrations can tell us about signal processing dynamics of synchronization in networks based on network structure alone [15], and hence it is crucial to understanding

the signal-processing tasks performed by this network.

2.4   Input trees, fibration symmetries and synchronization in a network

Conveniently, a *graph fibration* allows us to partition the graph in *fibers*. The name fiber comes from the theory of fiber bundles, which are a special case of fibration. Fiber bundles are the topological structure for the symmetries of the standard model. We further note that fibers are called *balance colorings* or *equivalent relations* in other branches of mathematics, dynamical systems and chaos. We use the term fibers that is more common in computer science, algebraic geometry and physics. In the case of regulation networks, these are sets of genes that are synchronized in their activity. This is the case for the blue nodes in figure 3, fibrations symmetries predict that these nodes will synchronize in the same gene co-expression patterns.

In order to determine the fibers we start by defining the *input set* I_i of node i as the set of incoming edges $e \in E_G$ such that $t(e) = i$ along with their respective sources $j = s(e)$. Figure 3b shows examples of the input sets of the nodes in graph G in Fig. 3b. It is easy to see that since nodes 1 and 4 have no inputs, their input trees consist of just themselves. Nodes 2 and 3, on the other hand, receive input from nodes 1, 2 and 4, which are therefore contained in their input sets.

The *input tree* T_i of node i can then be considered as input sets of input sets taken recursively. Input trees can be finite or infinite depending on the existence of the cycles in the network. Figure 3b shows a few examples of the input trees of nodes in graph G in Fig. 3A. It can be seen that the input set of node 2 is repeatedly attached to node 2 at every layer of the tree and this process is repeated infinite amount of times. As a result, input trees of nodes 2 and 3 are infinite, this is due to the self-regulation loop of node 2. An infinite input tree occurs anytime that a gene receives information from a strongly connected component of one (an autoregulated loop) or more (a cycle) genes.

More formally, for a given graph $G = (N_G, E_G)$ the input tree T_i of node $i \in N_G$ is the set of all pathways in G ending at node i [52]. Therefore, the input tree of a given node summarizes the regulatory pathways from the network that reach this node. This allows us to creates a classification of the nodes based on the 'history' of the signals they receive.

We then determine the nodes that belong to a same fiber by determining sets of nodes with *isomorphic* input trees. A *graph isomorphism* denotes a graph morphism whose inverse is also a morphism, i.e. a graph isomorphism is a bijective (one-to-one correspondence) graph morphism. Formally, a graph morphism $\tau : G \rightarrow C$, between graphs $G = (N_G, E_G)$ and $C = (N_C, E_C)$, is a graph *isomorphism* if and only if for every edge $(i, j) \in E_G$ there is an edge $(\tau(i), \tau(j)) \in E_C$.

Two graphs are said to be isomorphic if there exists an isomorphism between them. Fig. 3B demonstrates an example of two isomorphic input trees. Indeed, the topology of these trees is exactly the same, meaning that the graphs are the same except for a relabeling, and the isomorphism condition above is satisfied. The *graph isomorphism problem* attempts to determine whether two finite graphs are isomorphic. It is a very hard problem in computer science which is not known to be solvable in polynomial time nor to be NP-complete. Luckily, for fibrations, graph isomorphism is only needed between rooted input trees, and for trees the problem is polynomial.

A graph isomorphism of input trees defines an equivalence relation between nodes of the graph, and equivalence classes of nodes with isomorphic input trees. Reference [9] shows that these equivalence classes correspond to fibers: if two nodes have isomorphic input trees, they belong to the same fiber, there exists a fibration that collapses these nodes into one. Figure 3A illustrates this interesting connection: fibration $\varphi : G \rightarrow B$ collapses nodes 2 and 3, whose input trees are isomorphic.

The collapse of nodes in the fiber is interpreted as a symmetry. It corresponds to nodes being equivalent as far as signal processing in the network in concerned. Nodes in a fiber receive the exact same signaling 'tree', this makes the paths of signals rooted at them symmetric. This in turns makes the nodes in a same fiber symmetric in terms of signal processing or information flows in the network. In terms of an admissible set of equations attached to the graph, fibers lead to the existence of synchronous solutions for the nodes within the fibres [52, 40, 15]. This is called *cluster synchronization.*

This process of partitioning a network into sets of fibers with isomorphic input tress is also referred to as finding the minimal balanced coloring of the network. It seems necessary to point out that undirected networks can have multiple balanced colorings including some exotic ones, however, for the case of directed networks, given that order of signals is more clearly defined, this doesn't seem to be an issue.

2.4.1 The symmetry fibration: Collapsing a graph into its minimal base by surjective fibrations

The main reduction process is the application of the surjective minimal fibration, or *symmetry fibration*, which reduces the original network to its minimal base. Once the minimal balanced coloring has been found, by any algorithm (we implement our own [52, 51]), the network can be collapsed without altering the dynamics or information flow of the network. Given that all the nodes in a fiber have an identical history of inputs you can collapse all nodes from a fiber into just one single node with the input tree that these nodes share. This means that the corresponding pathways of information for that input tree are not lost, just that the redundant pathways are gone now. Instead of having multiple identical pathways you just have one. All of the symmetric synchronous nodes are then replaces with just one representative node per fiber. All of the output edges of any node in the fiber have to be added on the new representative node.

The network obtained as a result of collapsing the fibers is called the base, in this case the minimal base, since we are collapsing all of the fibers. This base network represents the reduced effective model network for the original system. And has the same original signaling flow but with no redundancies. DeVille and Lerman [15] have shown that any surjective fibration $\varphi : G \to B$ induces synchronization on nodes i and $j \in N_G$ if $\varphi(i) = \varphi(j) \in N_B$. Thus, for the case of a symmetry fibration, all nodes within the same fiber are synchronous. This guarantees that the dynamics for both the original network and the base network are the same, all the collapsed nodes dynamics are identical to the representative node they were collapsed into.

Importantly, this reduction is valid for any signaling-processing network when wanting to simplify the network size substantially without loosing the signaling flow of the network [52].

The base for *E. coli*'s TRN can be seen in Figure 7A after Step 1. An example of this collapsing is also shown on the fibers regulated by the SCCs in *E. coli* in Figure 6.

Synchronization requires that isomorphic input trees do not experience any significant communication delays which would cause asyncronicity and that the constants involved in equation 1 are approximately the same for all the genes in a fiber. This is not difficult to satisfy in TRNs where interactions depend mainly on the TFs and not so much on the binding site of the regulated genes. Small variations resulting from the mismatch of parameters appear to result in *weak symmetry breaking* that creates a slight reduction in the synchronization and correlation of expression levels within fibers [40].

It is important to note that the theory of fibrations only predicts the existence of these symmetric synchronized solutions. But not all synchronous solutions must be symmetric. More importantly, symmetries do not guarantee that the synchronous solution will be stable, and solutions may (in theory) be dynamically unstable [23, 64].

Thus, fibrations do not cover all dynamics in the original network, and guarantee existence but not stability. Fibrations cannot guarantee that these symmetric solutions are actually relevant dynamic attractors and not unstable.

Whether the synchronous solution is stable or not does not depend on the graph but on the type of dynamical model use to model each arrow in the graph. Thus, different stabilities can be obtained for different models, whether we use a Hill function or a linear interaction term or a step function, for instance, in the ODE. In fact, there are very interesting bifurcations that can exist for a given dynamical model, and bifurcation can be symmetry preserving or symmetry braking. Each fiber needs to be investigated separately for each model. The stability and bifurcation analysis of the circuits found here in the bacteria TRN are investigated in detail in a follow up paper [63].

2.4.2 Existence of the symmetry fibrations leads to co-expression of genes.

In TRNs a symmetry fibration can help us study the synchronized expression of genes with isomorphic input trees or, biologically, gene co-expression [39, 40]. The underlying assumption is that the gene regulatory input functions, as well as their parameters, are identical between all genes in a fiber. In biological reality, this is clearly not true: different genes (even with the same input edges) will show different gene regulation functions, mRNA lifetimes, etc, and so genes in a fiber will not show a strict synchronicity. However, we assume that these genes will still show correlated dynamics, and that the deviations from strict synchronicity can be described as a weak symmetry breaking [40]. Thus, we consider a simplified picture of TRNs in which this symmetry assumption for gene regulation functions holds.

The co-expression patterns obtained here are more general than traditional co-expression patterns in operons and regulons. Indeed, all genes in an operon with a single common promoter are in the same fiber.

Such operons can be thought of as examples of *"trivial"* fibers, see figure 2. The same applies to nodes that belong to only one regulon and share the same regulatory TF, they form a *"trivial"* fiber since they are only regulated by one gene in an identical manner. Generally speaking, symmetry fibrations allows us to find not only these trivial fibers but also broader co-expression patterns among genes that are far away in the genome and more complex patterns of synchronization. Particularly interesting fibers, shown in Fig. 2, are the Fibonacci fibers where the presence of a feedback loop between the fiber and its regulator (forming a a SCC) and a self-loop produce an input tree with a branching ratio of fractal dimension, as seen on figure 2, and composite multi-layered fibers, in which nodes that are not regulated by the same node are still synchronized because their regulators belong to a same fiber.

We have shown before [52, 53, 39, 40] that the use of fibrations in message-passing networks allows for the decomposition of the network into its fundamental signal-processing building blocks. A building block consist of the induced subgraph containing the genes in the fiber and the regulators that define it. We then classify them into $|n, \ell\rangle$ classes, where ℓ corresponds to the number of external genes regulating the fiber and n the number of cycles within the fiber. n can be an integer or fractal dimension, depending on if the input tree's branching ratio can be described by an integer number or not. The full list of fibers and their classification on *E. coli* can be seen on the SI from [52]. For *E. coli* and *B. subtilis*, all the different building block structures full under the classification of just 5 basic canonical structures shown in figure 2.

In summary, by studying the input trees of all nodes in a graph we can determine all the symmetries of the network in terms of signal processing. Specifically, the symmetries of a network are given by the equivalence relations induced by input tree isomorphisms. Therefore, symmetric paths can be removed while preserving the flow of signals, which ties concretely with the concept of fibration [9, 15] and its implications for the dynamics [52, 39, 15].

2.5 Injective Fibrations

An injective fibration can help us formalize the intuitive notion that under certain conditions the dynamics of an entire system may be driven by only a subset of its constitutive elements. This is formalized by *lemma 5.2.1* in Ref. [15], where it is shown that for an injective (one-to-one) fibration $\varphi : G \to G_2$ the dynamics of the bigger graph G_2 is driven by the dynamics of the smaller graph G. In fact G is a subgraph of G_2. This can be seen on Fig. 3 with the injective fibration from G to G_2.

The emphasis here is on the injective nature of the map φ. For a mapping to a bigger graph to be a fibration, like the one shown in Figure 3, it must satisfy the lifting property. This requires that all the edges in G_2 whose target node is an image from a node in G (i.e. $1', 2', 3', 4'$), can be uniquely *lifted* to an edge in G. This implies that no new edges are allowed to target any of the nodes of the original graph (i.e. $1', 2', 3', 4'$), satisfying the lifting property.

As a consequence, all the added nodes in G_2 (i.e. $5', 6', 7'$) must strictly be only targets of the image nodes. Hence signals flow only outwards from G, and so the dynamical state of the outer nodes is driven by the dynamics of the original smaller graph G. In other words, the subgraph G of G_2 drives the entire dynamics of G_2. This in turn guarantees that the dynamics of the original graph are preserved in the image graph G_2.

2.5.1 A k-core decomposition reveals the nodes that shape the network dynamics

An injective fibration leads from subset to set, but in order to reveal the minimal driving set of nodes of the network we must do the inverse of this mapping: from the entire set, we must obtain the subset driving the dynamics. This is done by applying a k-core decomposition to the network, which allows us to distinguish between nodes that shape the network dynamics and others that are just being driven.

The k-core decomposition of a network consists of 'peeling off' layers, formally called the k-shells of a network, by assigning a coreness index (k_s) to each node, corresponding to the respective shell they belongs to. The k-shell corresponds to the set of nodes with coreness $k_s = k$, the lesser the coreness k_s of the node, the more peripheral it is [33], as can be seen in Figure 3C. The coreness of a node captures the degree of the nodes it is connected to. For example, node b in Figure 3C has a smaller coreness ($k_s = 1$) than node a ($k_s = 2$), even though b has a higher degree of 5 compared to a's degree of 3. This is because b is connected

mostly to nodes with a degree of 1, in contrast to a that connects to nodes with higher degree, making it more *"influential"* [33] or central.

The coreness of a node is given by k if it belongs to the k-core but not to the $(k + 1)$-core [43]. For example, nodes having a degree of at least 0 belong to the $k = 0$ core (all nodes), node b therefore belongs to the $k = 0$ core and to the $k = 1$ core, as shown in fig. 3C, but does not belong to the $k = 2$ core so its coreness is $k_s = 1$. Taking the k-core of a network corresponds to removing all nodes with degree less than k, calculate the new degrees on the new subgraph, and remove again nodes with degree less than k, iteratively until all remaining nodes have a degree of at least k, this is shown in Figure 3D for finding the $k = 2$ core of the network. A node with coreness k has a degree of at least k, connecting to other nodes within the same core. Formally, the k-core of a network is the maximal induced subgraph, where the degree of every node within the k-core is at least k. (An induced subgraph corresponds to the resulting graph from taking a subset of nodes of the original graph and *all* the edges between them.)

To apply this concept to bacterial TRNs we must first extend it to directed graphs [43], where each node now is characterized by an *in-degree* and an *out-degree*, instead of the usual simple degree in undirected graphs. However, since we are interested in the direction of outward signaling flow, given that this case corresponds to the direction of regulation from one gene to another, we only need to consider the out-degree of each node. We are now interested in the k_{out}-core, which corresponds to the maximal induced subgraph where every node has at least an *out-degree* of k. This means that in this case we are iteratively removing the nodes with less *out-degree* than k.

In our case, we are only interested in genes that send any signals to other genes, we want to remove the ones that do not. Hence we want to remove the $k_{\text{out}} = 0$ shell of the network and obtain the $k_{\text{out}} = 1$ core, as the example in Fig. 3E.

In undirected networks, the $k = 1$ core contains the giant connected components of the network, this can be seen in Fig. 3C. Analogously for directed networks, the $k_{\text{out}} = 1$ core is composed of the *strongly* connected components and the nodes feeding them with signals. As shown in Fig. 3E the $k_{\text{out}} = 1$ core contains the SCC involving nodes 1 and 2 as well as node 4 which sends signals to it. This also shows that all acyclic directed graphs have a null $k_{\text{out}} = 1$ core.

In a sense we are trimming the frayed ends, or loose ends, of the network to unravel its core. In Fig. 3E we see the k-core decomposition of the graph G_2 from the injective map in Fig. 3A.

By Deville and Lerman's contributions [15], we know that when we have an injective fibration between two graphs $\varphi : G \to G_2$, the smaller graph G is the one that drives the dynamics for the entire system. The issue for us however is how to obtain the driver graph G given only G_2. We are proposing here that the k-core decomposition of a graph is the tool that allows us to perform the *inverse* injective fibration to find the driver sub-graph of the network G.

Given that by definition the k-core decomposition of a network is a maximal induced subgraph (see definition above), this guarantees that from the k-core decomposition of a directed graph we can obtain the full graph by way of an injective fibration: just adding the removed edges and nodes. Since we are taking the k_{out}, all the removed edges and nodes are outward facing of the core, and so this respects the lifting property to be a fibration.

When collapsing only to the $k_{\text{out}} = 1$ core without applying the symmetry fibration, one finds a subset driving the entire graph. However this may not necessarily yield the *minimal* subset, given that there might be some redundancy in the signaling flow of the resulting network. For example, in the case of a 2-node SCC whose nodes also belong to the same fiber, shown in Figure 3F, given that both nodes 1 and 2 have an *out-degree* of one, they belong to the $k_{\text{out}} = 1$ core of the original network. However, when applying the symmetry fibration first, they collapse into a single node with a self-loop and no *out-degree*, which implies that they no longer are part of the $k_{\text{out}} = 1$ core.

Hence, as input tree isomorphism tells us the correct way to apply a fibration and collapse the network while preserving signaling flow, the k-core decomposition, and in particular the $k_{\text{out}} = 1$ core, gives us the correct *inverse* fibration to reduce the network into its minimal set of nodes driving the dynamics.

2.6 Broken symmetry circuits: hierarchy and identification

Broken symmetry circuits act as circuits performing basic logical computations in biological networks, such as memory storage and timing via oscillatory behavior [39]. They are obtained by breaking the symmetry of
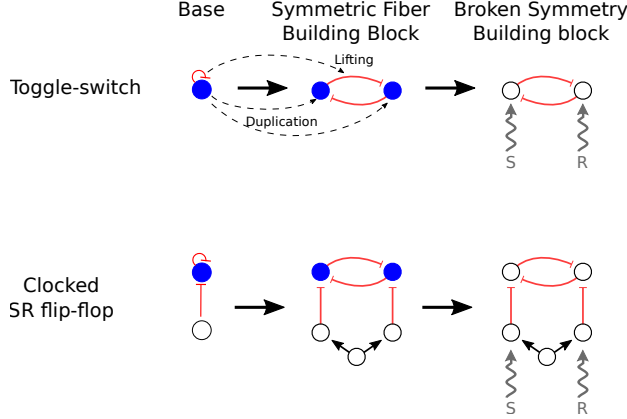
Figure 4: Broken symmetry circuits and duplication process. Starting with an initial simple structure a gene duplication process can create a symmetric fiber structure, analogous to a lifting process. The circuit formed depends on the initial structure that is replicated. For each circuit, the symmetric form is shown on the center, while the broken symmetry process is shown on the right. The *set-reset (S-R)* inputs break the symmetry by sending different regulations to an otherwise synchronous pair of nodes. The *S-R* inputs can be any different nodes sending different signals or can be a same node sending different signals to the nodes in the fiber.

a symmetric building block. The symmetry breaking occurs by adding regulators that do not regulate the nodes in the fiber in a symmetric manner, i.e. nodes within a fiber start being regulated differently, as shown in figure 4.

The structures whose symmetry gets broken (seen on Figure 4) are obtained from a *'gene duplication'* process on the base of the basic building blocks (see Figure 2). After a gene duplication in evolution, a cell would end up with two paralogue copies of a gene. This duplication process can *'open up'* the base of a fiber building block, identical to how the lifting process opens up a fiber from the base into the full set of synchronous genes. If the duplication works in such a way that the obtained duplicated circuit, the replica circuit, still preserve the same input relations but now with a number of synchronous genes where before there was just one, then it is analogous to a liftying process. Breaking the symmetry of this replica circuits however, gives rise to logic circuits. In fact, gene duplication may be an explanation as to why TRNs exhibit so much symmetries [52], as well as providing a suitable method for creating this logical circuits in the networks, as will be discussed in the **Discussion**.

Duplicating a self-inhibiting gene in such a way that results in two mutually repressed (MR) genes forms a two node negatively auto-regulated (NAR) fiber (a fiber that auto-regulates itself in an inhibitory manner) as the one shown in the upper part of Figure 4. When the input to the two genes is differentiated by introducing different regulators to each node and breaking its symmetry, the resulting circuit corresponds to a structure analogous to a *flip-flop* in electronics [66] with the different inputs for each gene being the *'set' (S)* and *'reset' (R)* switches. This circuit corresponds to the toggle-switch [20, 39] and it is able to store one bit of information given that it has two possible stable and reciprocal states: one gene being expressed and the other one not, and its reciprocal case. Even when the symmetry is restored and both inputs return back to being identical, the circuit remains in its broken symmetry state and hence stores the previous state as a bit of information. It is possible to switch between the two states by toggling the *S-R* inputs to the circuit, hence why this is referred to as a two-way switch.

An analogous symmetry breaking process with the circuit generated from a Feed-Forward Fiber (FFF) building block instead, shown on the bottom part of Figure 4, gives a circuit resembling a clocked *SR flip-flop* [39, 66], which basically acts as a more complex *flip-flop* or toggle-switch. A FFF consists of a Feed-Forward Loop (FFL) motif (a three gene structure of genes X, Y and Z, where gene X regulates both Y and Z, and gene Y also regulating Z) [44] with an extra self-regulation on gene Y. This self-regulation in Y induces synchronization on both genes Y and Z, since it induces their input trees to be identical [52, 39]. Depending on the signs of both regulations by X and Y, the inputs received by gene Z can be coherent or

incoherent, classifying the FFLs as either coherent and incoherent [44, 1] and the FFFs as SAT-FFF or an UNSAT-FFF [39], respectively. From their dynamical equations the UNSAT-FFF solution synchronizes and oscillates [39] meaning this circuit could work as a clock component.

This process can be continued with more complex fiber building block structures (Fig. 2), leading to a hierarchy of broken symmetry circuits as shown in ref. [39], for example with Fibonacci fibers to give Fibonacci circuits, analogous to a JK flip-flop in electronics. However, these more complex circuits were not observed on either TRN studied in this work.

Crucial to the dynamics of these circuits are feed-back loops between different genes. This implies that the circuits are always embedded into the SCCs of the network. Given that the SCCs are preserved after our reduction method, we know that we are not losing any logical components of the network as we reduce it. This means we can interpret the SCCs of the network as the modules where the logical computations are performed.

To find the circuits mentioned above, we run an algorithm looking for the induced subgraphs of the minimal network whose connectivity is identical to the logic circuits we are looking for. The algorithm is explained in more detail in the SI of ref. [39] and corresponding codes can be found at https://github.com/makselab/CircuitFinder. Briefly, the algorithm consists of two steps: 1) find the subgraphs of the minimal network isomorphic to a broken symmetry building block and 2) only keep those subgraphs that are induced. Some of the observed circuits however, have a slightly different topology due to self-regulations of some genes in the circuits, so their dynamical behavior might be different.

2.7 Identifying simple directed cycles

After reducing a network via k-core decomposition as described in section **A k-core decomposition reveals the nodes that shape the network dynamics**, the remaining nodes have an output degree of at least one (all *null* pathways ending at nodes with no-outputs have been removed). Hence, the SCCs are left intact during the k-core decomposition. Given that all the logic circuits belong to the SCCs, in order to study the interconnectedness and interplay between these circuits we take a look at the cycles present in the minimal TRN. For this, we look for all the simple directed cycles in the network (a simple directed cycle is a closed path that crosses each node just once, except for the initial/final node). This is related to the concept of Betti Numbers in simplicial homology [54], where the k-th Betti number illustrates the number of k-dimensional holes in a space. A cycle in this sense describes a type of topological hole. In particular, in the case of undirected graphs the first Betti number $b_0 = |C|$ where C corresponds to the number of connected components, while the next Betti number b_1 gives the number of simple cycles [5].

In directed graphs, determining the number of cycles is an NP-complete problem [26]. Both networks studied here are small enough to be analyzed using state-of-art techniques producing output in a matter of minutes. The employed algorithm is loosely based on *Johnson's algorithm* [30]. It starts by breaking the network into SCCs and searches for cycles within each one. Each component is analyzed by 1) enumerating the nodes in the SCC, 2) choosing one node (the initial/final node of the cycle), 3) looking for the outgoing neighbors of this node, and 4) looking for all the simple paths (paths without repeating nodes) back from each neighbor to the chosen initial/final node. Since a self-loop or buckle, just connects a node to itself in a cycle of length 0, they don't really contribute to the computational machinery and hence we ignore them for our cycles analysis.

By definition, a SCC is a subgraph in which every node is reachable from every other node, Therefore, a SCC is basically a compound structure of cycles intertwined with each other. For example, on the extreme case where every node directly connects to every other node: every pair of nodes form a cycle, every trio of nodes is also a cycle, so on and so on. This implies that there will be simple directed cycles present in any SCCs, in which some signal will cycle through them. In fact, in TRNs most of the different cycles observed share nodes, for example, given two nodes that form an auto-regulation loop, most of the time there will be other longer cycles connecting them as well, as illustrated in Fig. 7C. One possible function of these longer cycles could be to serve as a form of longer-term memory.

3 Results

3.1 A method for reducing the TRNs to their computational core

We developed a framework for reducing the complexity of Transcriptional Regulatory Networks to better understand their structure and how it allows for signal processing. Based on graph fibrations, we develop a stepwise procedure to reduce the TRN to its computational core in order to better understand the structure of the network and how it informs us about the decision making process of the cell. We call this method: "Complexity reduction by Symmetries" (ComSym). Figure 1 shows the reduction procedure for the case of *E. coli*: the TRN shown on the left is reduced to the simpler, better understandable structure on the right that elucidates how the network works.

ComSym provides insights about the collective behavior of the network based on its topology. The process can be applied to any directed network regardless of the model used to describe the underlying dynamical system, given that it does not depend on the actual form of the admissible equations on the graph [23, 64]. The procedure consists of five steps:

1. graph reduction via symmetry fibration,

2. reduction via k-core decomposition by inverse injective fibration,

3. decomposition of the core network into strongly connected components,

4. identification of broken symmetry building blocks in the core network, and

5. identification of loops in the core network.

The first reduction step, *'collapsing'*, removes symmetries in the signaling flow in the network originating from fibration symmetries. This step is based on lemma 5.1.1 from Ref. [15] which proves that the dynamics of a network is preserved when all symmetries are eliminated by a surjective (onto) graph fibration. The reduction of the network in this step is achieved by applying the symmetry fibration to the original network. This consists of collapsing all the fibers to a single representative node for each fiber and obtaining the minimal base.

The second reduction step, *'pruning'* the loose ends in an iterative way, makes use of the direction of the signal flow in the network. The k-core decomposition of the network identifies an "outer" layer (shell) of nodes that do not send signals to the ("inner") core of the network. Lemma 5.2.1 in Ref. [15] shows that the dynamics of the nodes in the "outer" layer is driven by the dynamics of the (inner) core network. Therefore, dynamical behavior of the core network can be studied separately and further used to scrutinize the dynamics of the "outer" layer. Reducing the network to its core is performed by applying the inverse injective fibration. This step can be thought as trimming the loose ends of a tree. The removed edges are the leaves that send information to other parts of the bacteria, like the metabolic network via genes that express enzymes.

These two reduction steps yield the core subnetwork that controls the dynamics of the entire system. Such reduction can dramatically reduce the network. For example, the network of *E. coli* is reduced from 1,843 genes to only 42 nodes. This core reduced network is then decomposed into its strongly connected components, SCC, plus the controllers or external regulator nodes that send signals to the SCCs but do not receive any signals back (otherwise they will be part of the SCC by definition), thus regulating or controlling the components of this reduced network. These components correspond to the strongly connected components (SCCs), subnetwork components of the network where every node can be reached from every other node.

After pruning the loose ends of the network, all the paths that end at nodes with no *out-degree* are lost, meaning that all the remaining paths self-cross at some point. For this reason we want to understand how the network decomposes into SCCs, it could very well be that there would be no structure between the SCCs of this reduced networks. However, we find very interesting structures connecting the SCCs in the reduced networks.

Then, the core network is decomposed into strongly connected components plus single nodes regulating them. This step is based on the following insight: in any network where there are cycles present, there is at least one strongly connected component that does not receive any inputs from the other strongly connected components. Indeed, if there were two strongly connected components in the network for which there existed back and forth paths between them, these two components and all the nodes on this path would be strongly

connected. Therefore, the behavior of strongly connected components with no inputs can be studied separately and further recursively integrated to study the components that receive input from them.

The final steps in ComSym consist in searching for fiber building blocks [52], symmetry breaking building blocks [39] and loops in the core network [57].

3.2 Application to bacterial TRNs

To demonstrate the use of our method, we applied it to two of the best studied bacterial TRNs, the networks of *E. coli* [59, 49, 67, 45] and *B. subtilis* [22, 19]. The stepwise reduction of the *E. coli* TRN is shown in Figure 7A. Table 1 shows how the number of nodes decreases in each step.

The TRN *E. coli*'s network as downloaded from Regulon DB contains 4690 genes. The majority of these genes expresse proteins that does not interact with any other gene. These genes are isolated thus are not part of the network so we do not consider them in our analysis. This leaves us with the 1843 genes involved in the TRN. We then collapse the operons into single nodes to avoid *"trivial"* fibers, describing genes in the same operon. Operon with internal promoters were split into transcription units (TUs), which were then kept as separate nodes. This trivial reduction, which is in reality a part of our step 1 of collapsing, shrinks our initial 1843-genes TRN to 879 nodes. This operon collapsing was done for the sake of analysis, to avoid looking at trivial operons which are very well known structures but for the sake of our method is not strictly necessary.

Below, we will first describe the two steps of network reduction in detail. Then, we show how to use the method to identify logic circuits in the core network interpreting it as a computational core machine, we discuss hierarchies of broken symmetry circuits, and describe simple cycles in the core network.

3.2.1 Network reduction step one: collapsing nodes via a symmetry fibration

We first obtain all the fibers by a minimal balanced coloring algorithm. The algorithm starts by giving all the nodes the same color, except for the nodes with no inputs since biologically there is no reason for them to be synchronous. Then the color of the nodes are re-calculated: nodes are given the same color if they receive the same amount of inputs for every color they receive. For example, two genes that receive both one blue and one red input (just to say some colors as examples) are given a same color. A third node that also receives one green input would not be given their same color. By changing the colors, the color-inputs of the nodes change as well. The colors are then re-calculated again based on the new color-input relations. Once the coloring is stable this means the coloring is balanced and minimal, and the fibers have been found. See [52] and its SI for more information, also [51]. The code with our implementation for this can be found in our lab's github: https://github.com/makselab.

Once the minimal balanced coloring algorithm is run, the fibers are found by the set of nodes that share a same color. A fiber along with the regulator(s) that define it are the fiber building blocks. For both *E. coli* and *B. subtilis* we found a nice hierarchy of five basic types of building blocks, shown in Fig. 2. Through this 5 basic building block structures all the symmetries in both model bacteria can be constructed. Figure 5 show all the different possible configurations from the building blocks observed in both *E. coli* and *B. subtilis*.

The first and simplest of this structures, we just refer to as trivial fibers, is the case where there is no self-loop in the fibers so the input-trees of the fibers are simple. This are the fibers that you could sort of *'trivially tell'* by simple inspection that should be synchronous. They can be subdivided by the number of ℓ regulators to the fiber. The second structure corresponds to when there is one self-loop in the fibers, we call these Feed Forward Fibers (FFF). They are further subdivided again by the number of ℓ regulators to the fiber, with the note that in this case they could have no external regulator and have the genes be synchronous by account of one gene that regulates the rest and *also* regulates itself in the same manner. The 1-FFF actually corresponds to the famous feed-forward loop but a self-loop added on the *'middle'* that makes it synchronous. The next structure, one of the most interestings, we call *Fibonacci* on account on how introducing a link from the fiber back to the regulators gives rise to a fractal dimension. The $n = 2$ building block is defined, self-evidently, by there being two self-loops. Something very important about this building block is that the different combinations of edges types (activation or represssion) give rise to different type of logical circuits. For example, if both loops are inhibitory this is the toggle-switch and the symmetry breaking of this structure is what determine the logical output of the circuit, with the symmetry breaking inputs being the SR-inputs to the toggle-switch circuit. Accordingly, we only found symmetry broken versions of the $n = 2$

with both edges being repressive. Another example is the Smollen oscillator corresponds to the $n = 2$ with one activation and one repression loop.

Applying the symmetry fibration to *E. coli*'s TRN leaves it at just 555 nodes, 30% the size of the original network, as seen on table 1. As mentioned before, collapsing the operons is not a necessary midstep, Step 1 could have been directly from the full 1843 network to the reduced 555 nodes base network. This reduced network still preserves the same dynamics as the original network, on account on Deville and Lerman's results mentioned before [15], with all the redundant information pathways collapsed into just a single one.

3.2.2 Network reduction step two: trimming the network via a *k*-core decomposition

Given the definition in the *Methods* section **Injective Fibrations**, we see that the $k_{\text{out}} = 1$ core of the network corresponds to the minimal subgraph driving the entire system, and contains the SCCs which are the logical computational modules of the network. Figure 7 shows the application of the *k*-core decomposition, the second step in our reduction process, to *E. coli*'s collapsed TRN from the first step.

The *k*-core decomposition allows us to determine the nodes that do not send signals, or that send signals to a path that ultimately do not *'compute'* and just transmit signaling chains. For example enzymes, which only receive regulations from TFs but do not regulate any other gene since their role is to catalyze metabolic reactions.

At the end of the step what remains are the SCC, the computational 'hubs' of the network, their connections and the nodes connecting them between each other, or regulating them. This reveals the structure of the core the network, or the minimal network that is responsible for driving the dynamics of the entire network. The simplest possible structure would be to just have one SCC and nodes controlling it, akin to a 'trivial' structure, however for both studied bacteria the structure of the core network is revealed to be a rich structure connecting a number of SCC in very interesting ways, much than expected for the null-model, as is shown later in this work.

3.2.3 Large-scale structure of the core TRN: Strongly Connected Components (SCCs) as "signal vortices"

After the core of the network has been determined (i.e. the minimal network driving the dynamics, as shown for *E. coli* on Figure 7), we analyze it first by splitting it into components defined as the strongly connected components (SCCs) of the core graph. A SCC is formally defined as an induced subgraph in which every node is reachable from every other node through a directed path [17, 10, 3]. The simplest example of this is a two node feed-back loop as the one between nodes 1 and 2 in Figures 3E and 3F. As we will discuss next, a simple feed-back circuit between two nodes can form a logic circuit, depending on the type of the regulations this can be a either a toggle-switch [20], an oscillator [65] or a lock-on circuit [20, 65] (see also Fig. 2). This is one of the reasons why the SCC as components are important for the breakdown of the core network, because they contain the logic circuits within the core of the network. The SCCs of *E. coli* are encircled in Figure 7 illustrating the reduction steps of the TRN, as well as showing the symmetry breaking inputs into one circuit embedded in SCCs.

Among the 6 SCCs, the modules of the core, we obtain one with 11 nodes which mostly regulates the cell's *pH* and *stress* response (we will refer to it as the *pH* SCC), one with 5 nodes (the *soxS* SCC). And the rest with only two nodes: *crp-fis* serve for carbon utilization, *marA-rob* control a number of genes

Reduction step	Gene count	%
Step 0.1: Full TRN	1,843	100%
Step 0.2: operon-TRN	879	48%
Step 1: Collapsing Fibers	555	30%
Step 2: Pruning	42	2%

Table 1: Reduction count. Full *E. coli* genome is 4690 genes. The first reduction of operons was performed just for analysis methods to avoid seeing all the *'trivial'* operon fibers, this is in reality just a part of Step 1.

involved in resistance to antibiotics, *uxuR-exuR* which are involved regulation of transport and catabolism of galacturonate and glucuronate and *galR-galS* (relating to import and catabolism of galactose).

In Fig. 6 we can see the fibers regulated by the SCCs of the *E. coli*'s Minimal TRN and see how the base of this subnetworks look like. Perhaps unsurprisingly we see that *crp-fis* regulates the biggest fibers. Also of interest is that there are some fibers that are jointly regulated by two SCCs and that the *uxuR-exuR* and *galR-galS* do not regulate any fibers of their own although they do regulate other genes and operons.

In the past, modularity has been used as a ways to try to partition these networks and find some sense in their structure. However as we have shown, the strongly connected components not only make a very interesting structure of the minimal TRNs, along with knowing that the logical circuits for these networks must be found embedded in the SCCs, but they also seem to be divided in biological functions as well. And so, having two genes belong to the same SCC seems to be of more weight for them to have a similar biological function than having them be part of some cluster result of a given modularity partitioning of the network.

The *crp-fis* SCC works as a type of master regulator, controlling the rest of the SCCs and being regulated by only two external outputs: the *cra*-fiber and *ihfAB*.

The *galR-galS* and the *uxuR-exuR* SCCs receive signals from *crp-fis*, but do not receive or send signals to the rest of the SCCs. They compute their state solely based on *crp-fis* SCC's input and then send their corresponding outputs to the genes that they regulate.

The other SCCs are arranged in the shape of a feed-forward motif: *crp-fis* SCC feeding the *soxS* SCC and the *pH* SCC, with the *pH* SCC also receiving from the *soxS* SCC and another similar structure with the *marA-rob* SCC in the same role as the *pH* SCC: receiving from both *crp-fis* and *soxS*. The overall structure of the computational minimal core of the *E. coli*'s TRN corresponds to two *feed-forward* structures between the SCCs.

3.2.4 Small-scale structure of the core TRN: logic circuits

Since the inception of synthetic biology and the first designed genetic circuits two decades ago [20, 18, 12, 32], it is known that simple genetic circuits are able to perform basic logical operations necessary for any computational device, such as memory storage and time-keeping [14, 66, 70, 32]. Such circuits are constructed using feedback loops, both positive and negative, [70, 14] and are executed by synthetic switches and oscillators designed from simple components such as interacting genes or protein-protein interactions.

For *memory storage* in particular, the two most prominent designs are the *toggle-switch*, a bi-stable two-way switch analogous to an electronic flip-flop which functions as a binary memory [20, 39], and a *lock-on* "permanent" memory, a well studied simple genetic circuit consisting of a positive auto-regulation (PAR) feedback loop, which works as a bi-stable one-way switch circuit sustaining two stable states: both genes inactive or both genes active after either one has been activated [70, 1]. In contrast to the *toggle-switch*, the *lock-on* is a one-way switch, once the circuit switches to the activated case it is not able to turn to its previous state. This type of *lock-on* circuit would likely take a role in developmental processes characterized by a state-transition, such as apoptosis (programmed cellular death) [70].

Regarding oscillators, one of the most basic circuits with the oscillatory behavior is a purely negative feedback loop (NFBL), comprised by two genes A and B, A inhibiting B while B is activating A ($B \mapsto A$). This circuit by itself could functions as a pulse generator since it is only capable of sustaining damped oscillations [37, 1], however Refs. [21, 1] observed that in the presence of noise it sustains oscillations with

operon-TRN breakdown	Gene count	%
operon-TRN	879	100%
Nodes in fibers	416	47.3%
k_{out} shell (not in fibers)	431	49%
Nodes in SCCs (not in fibers)	20	2.3%
Connectors (not in fibers)	12	1.4%

Table 2: Breakdown of the operon-TRN network. Step 1 collapses the 416 nodes in fibers into just 92 fibers, to give the Collapsed-fibers 555 node network. Step 2, removes all the Shell nodes and 82 of the fiber-collapsed nodes, this leaves only the 42 nodes present at the Minimal TRN of *E. coli*
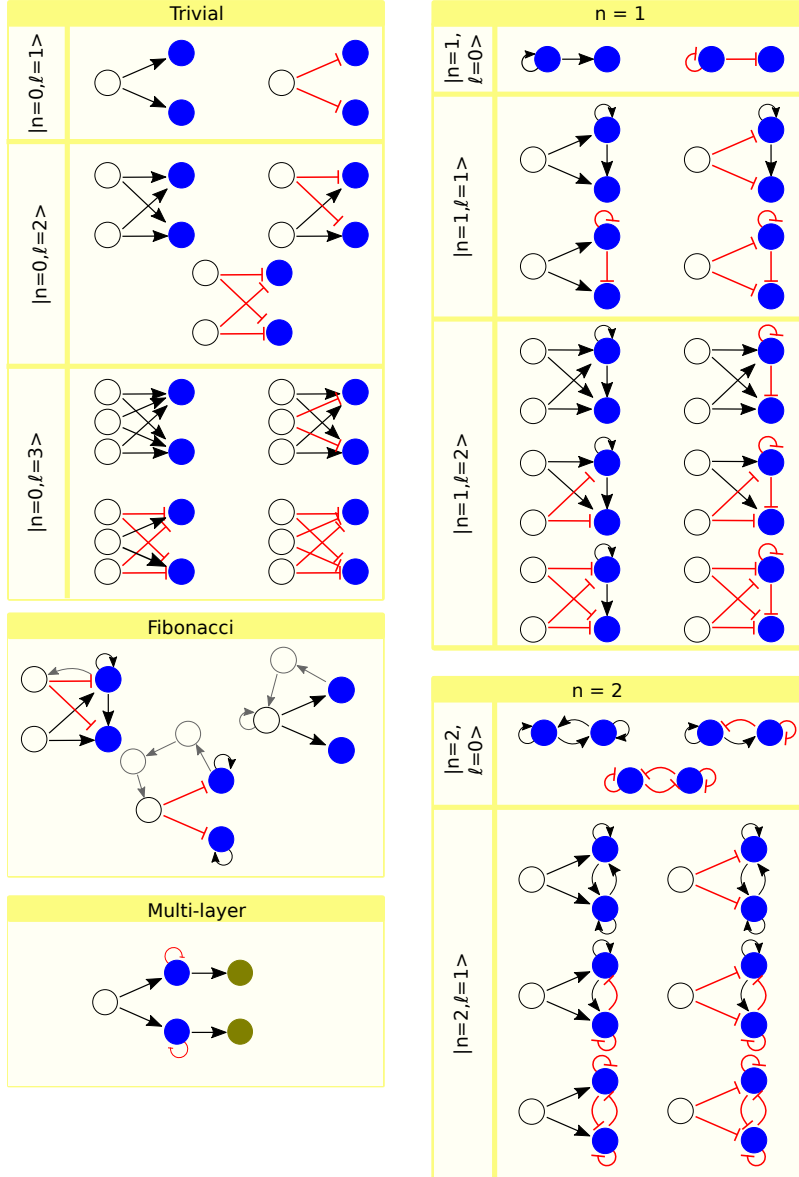
Figure 5: Possible circuits of the observed building block structures from *E. coli* and *B. subtilis*. We take the observed $|n, \ell\rangle$ classes in both bacteria and show all the possible combinations of activation and inhibition regulations for each class, i.e. all possible configurations which would still have a symmetric pair of nodes. In order for symmetry to occur the pair of synchronous nodes must receive an identical input tree. For the $n = 1$ cases, this can occur by a node with a self loop also regulating the other node in the fiber as shown, or alternatively by both nodes having a self-loop.

a reliable frequency but ill-defined amplitude. Some simple additions can be made to this basic structure to improve its oscillating behavior. For example, Refs. [57, 1] showed that from an analytical standpoint the addition of an activation self-loop in gene B provides an amplified negative feedback loop, however only damped oscillations have been seen *in vivo* [57]. Furthermore, addition of an inhibiting self-loop in gene A gives a *Smolen oscillator* which exhibits sustained oscillations [65, 57] in a robust and highly tunable manner.

Remarkably, we find the presence of circuits closely resembling of all these circuits in the minimal network driving the TRN. This invites to understand this minimal network as a logical computational machine. We systematically look for these circuits capable of logical computations in the minimal driving set of the network.
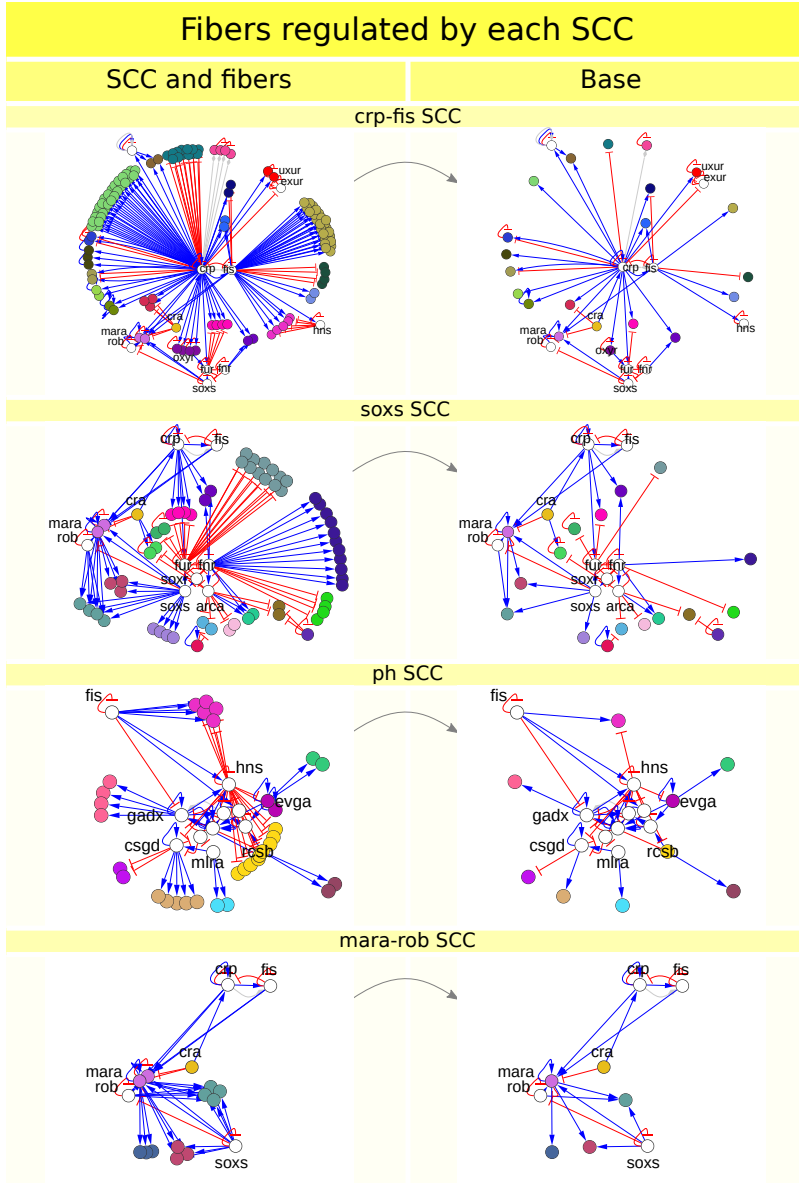
Figure 6: Example of a symmetry fibrations applied to the SCCs and the fibers they regulate in *E. coli*'s operon TRN. On the left, genes that belong to the same fiber share the same color. On the right all the fibers have been collapsed to a single representative node per fiber. Nodes shown with labels are nodes belonging SCCs or regulators to them. It is interesting to note that quite a lot this fibers are actually regulated by not just the nodes of one SCC but by two SCCs. For example, in the second row for the *soxS* SCC there can be seen two fibers between this SCC and the *mara-rob* SCC in greenish and brownish colors respectively. The same thing occurs with two other fibers shared with the *crp-fis* and *soxS* SCCs in pinkish and purple colors. Out of the 6 SCC, the *galR-galS* and *uxur-exur* SCCs do not regulate any fibers of their own and thus do not appear on this figure. Blue edges with arrows represent activation, red edges with bars represent inhibition and grey edges with rhombuses represent dual regulation

Since these circuits can be artificially constructed to perform computations, it is reasonable to expect to observe them, or some close variation, at the core computational subset of the network. We would expect to find memory storage circuits as well as oscillating circuits for time-keeping. In the case of the TRN of simple model bacteria, we would expect to observe the more simple forms of these known genetic circuits

from synthetic biology, which is indeed the case, as will be shown next. Remarkably, these circuits can be understood by the concept of a broken-symmetry fibration, introduced in Ref. [39], as discussed in **Broken symmetry circuits: hierarchy and identification**.

3.3 Transcriptional Regulatory Network of *E. coli*

3.3.1 Large-scale structure of the *E. coli* core TRN: signal vortices

The structure of the core SCC network is shown in Fig. 1B. The system of SCCs represents the smallest computational subunits which cannot be reduced further neither by the fibration symmetries nor by smaller strongly connected components. Thus, this structure represents the "minimal TRN" structure of the cell. The central subunit of this minimal TRN is the carbon SCC, which transfers information downstream to the other two main SCC components for pH and stress regulation. These two SCCs are connected in a forward manner, forming a feed-forward loop representing the core of the genetic computing system, thus capturing the minimal TRN. Within these three major connected components, symmetry-broken memory and oscillator circuits are found: the information travels along cycles turning on and off the toggle switches that store the memory in their states. We will show this in the next section.

We find a rich interaction between the network SCCs as well as the important role played by feed-back loops both in determining the SCCs and the circuits within, compared to previous observations [45]. Following our method, all genes in the TRN can be classified with regards to the function they perform computationally in the message passing dynamics. Each gene in the TRN belongs either to a fiber or to some logic circuit or sends inputs to logical circuits. Most of the external regulators of SCCs are directed towards logic circuits serving as the inputs for their computations.

The general flow of information looks like this: external signals enter the SCCs, and signals then emanate outward from the *crp-fis* SCC to the 5 other SCCs, where it is fed to the logic circuits. Then the output is communicated outwards to the fibers in the periphery of the network as shown in Figure 7A.

3.3.2 Circuits Present

Inside the SCCs of the TRN we found a variety of genetic circuits that closely resemble logic circuits designed and implemented in the synthetic biology literature. In total 12 different pairs of genes where found to be involved in a number of possible logic circuits, see Fig. 8 for a depiction of the full symmetry breaking for all circuits in *E. coli*.

We found three circuits resembling toggle switches: each of them consists of two mutually repressed (MR) genes, but with different self-regulations. Among them are the SCCs *galR-galS* and *uxuR-exuR*. For both of them, their only input gene is *crp*, which means it could function as the logical *S-R* input selecting the state for the circuits. Both of this circuits present additional negative auto-regulations in each gene (see Fig. 8), so their dynamics varies compared to the classic toggle-switch design.

In the case of *uxuR-exuR* cycle, with the regulations of *crp* this circuit then becomes the *Mutual Repression Network with Negative Autoregulation* studied by Hasan *et al.* [28]. This circuit can show two distinct stable states and may therefore serve as a memory: when *crp* is active, it can induce a state in which *uxuR* is expressed while *exuR* is repressed. The third possible toggle-switch-like circuit is between *csgD-fliz* in the *ph* SCC, shown in figure 7, with numerous possible ways for its symmetry breaking to occur, as can be seen in 7B. This circuit contains a positive autoregulation. As shown in [41], this allows for two stable states, making it possible for it to function as a memory device.

For NFBL (oscillator-type) circuits we observe 4 possible circuits: $rob \mapsto marA$ a SCC by itself; $soxS \mapsto fur$ in the *soxS* SCC; and $gadX \mapsto hns$ and $cspA \mapsto hns$ in the *ph* SCC. All of these are autoregulated, but the autoregulations in $gadX \mapsto hns$ figure 7) actually makes it a Smolen oscillator, the more robust type oscillator [65].

There are also three pairs of nodes that can show various behaviors given that they can send various types of regulation messages between them. For example, *crp* can send either an activation or repression signal to *fis*, which means that *crp-fis* can be a MR circuit (toggle-switch type) or a NFBL circuit (an oscillating type), possibly even a Smolen oscillator given its auto-regulations, see SI. A similar thing occurs for *fnr-arcA* in the *soxS* SCC, which can be either. Lastly *gadW-gadX* in the *ph* SCC, in which both genes send both
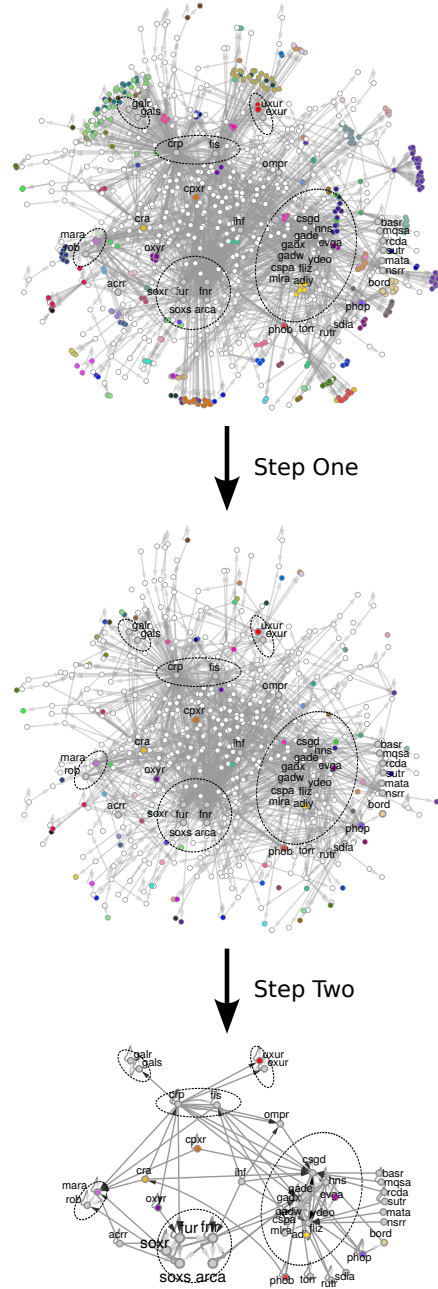
Figure 7: Network reduction of *E. coli*'s TRN. We start with the same network as in the left of figure 1, rearranged to show the outward flow of signals and with genes in the same fibers colored the same. SCCs are marked by ellipses, names shown are only for the genes belonging to the core of the network, obtained after the reduction. Most of the genes belonging to fibers are located in the periphery of the network. Various nodes with notably high out-degree in the network don't belong to the core network. *Step one* of our procedure collapses all fibers into one representative node, resulting in the base network from the symmetry fibration.*Step two* removes all the *null*-paths ending at nodes with no output via the *k*-core decomposition, resulting in the core of the network with only 42 nodes. The *crp-fis* SCC control all other SCCs, nodes outside SCCs are controllers to them.

activating and repressing signals, can be a MR, a NFBL or a PAR feedback loop such as in a 'lock-on' circuit, on top of this, one of the possible NFBL configurations includes a Smolen oscillator.
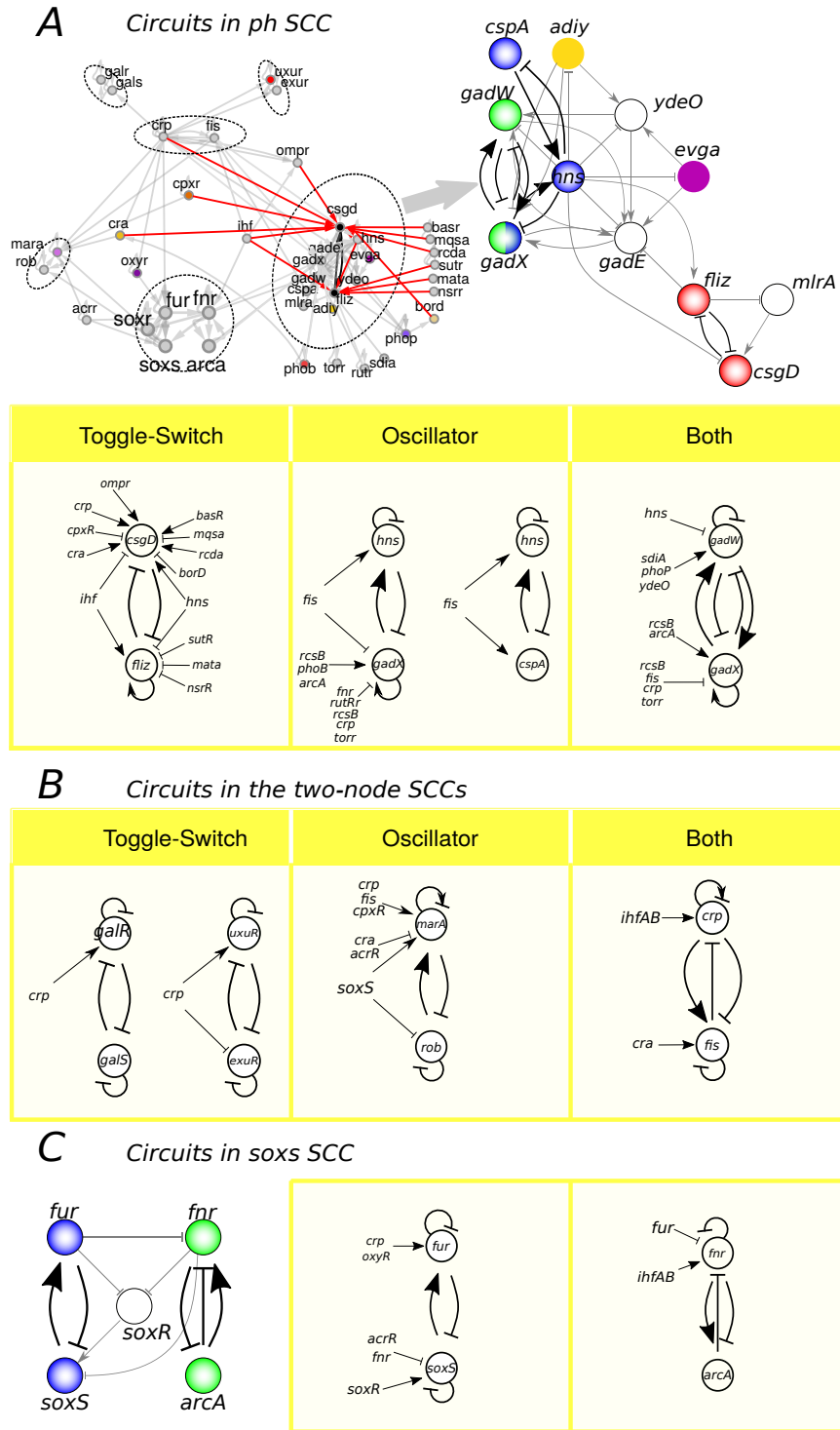
Figure 8: All circuits found in *E. coli*'s TRN. **A** we show the biggest SCC, in charge of mostly pH responses, and the circuits embedded in it. *E. coli*'s minimal TRN is shown with red links for the symmetry breaking inputs to the toggle-switch *fliz-csgd*. **B** the two-node SCCs and **C** the *soxS* SCC and its circuits. Nodes involved in toggle-switches are colored in red in the SCC depictions, oscillating nodes in blue and nodes in circuits that can be either in green. For every circuit, the incoming signals that break the symmetry are shown.
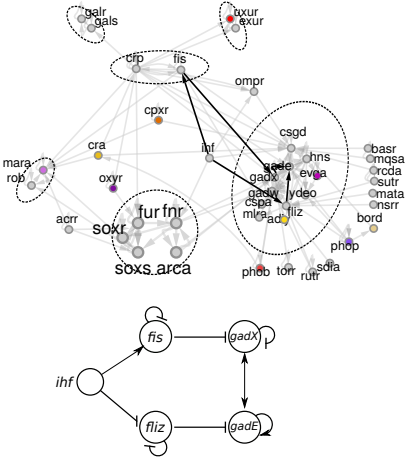
Figure 9: FFF circuit connecting the main SCC *crp-fis* to the *pH*-SCC. On the bottom we show the isolated circuit.

More surprisingly, we found FFF circuits, shown in figure 9 that connect the *pH* SCC to the master regulator *crp-fis* SCC and, through two different paths, to the *soxS* SCC, remarkably, the three FFFs are regulated by the same clock: *ihfAB*. It is worth noting that for the three FFF circuits the underlying feedback loop is a double-positive auto-regulation (PAR) feedback loop, which works as a bistable *lock-on* circuit, however the circuits are actually inhibiting the PAR.

3.3.3 Cycles

In total we found 41 simply directed cycles in the minimal core of *E. coli*'s TRN. Four of them being the two-node SCCs, 5 are located in the *soxS* SCC and the remaining 32 to the *ph* SCC. Each of the cycles contains a pair of nodes in a logic circuit, meaning that all cycles longer than 2 nodes pass through two nodes that are also connected by a logic circuit, all logic circuits themselves are of course two-node cycles.

For example, in the case of the *soxS* SCC we observe 2 two-node cycles (circuits *soxS* $\mapsto$ *fur* and *fnr-arcA*), the remaining 3 cycles in this component all pass through *soxS* $\mapsto$ *fur* and as such can be considered longer loops from *soxS* to *fur*, this is shown in Figure 7C. There are numerous cases in which the cycles even cross through multiple nodes that are connected by a logic circuit each other, this can also be seen in Fig. 7C as well, where the longer loops cross through *gadE-gadW*, *gadW-gadX*, and *gadX-hns* all of which are part of different logic circuits. In a way, all the loops shown can be considered loops of various lengths between the circuits *soxS* $\mapsto$ *fur* and *csgD*−*fliz*. A full list of all the cycles is provided on a separate file and also available at the repository https://github.com/makselab..

We are looking for these cycles since they are a form of longer memory between the logical circuits. They correspond to different ways of regulating these logical circuits.

3.3.4 The *E. coli* minimal TRN as a computational machine

Let us summarize our findings about the *E. coli* TRN. The two primary components of any computer are flip-flops (toggle-switches) and oscillators, both of which we found examples in the minimal TRN. Thus, the TRN can be seen as a computational device where the memory is stored and controlled by broken symmetry circuits within the 4 major SCCs (There are two extra two-gene SCCs that only receive information from the carbon SCC). The flip-flops in the SCCs control the turning on and off of a set of symmetric fibers representing clusters of genes displaying coherent synchronization in gene co-expression. The "information" of this computations from the flip-flops is then transmitted to other parts of the cellular network by way of the fibers. The switching of the flip-flops between their stable states (i.e., zero and one) is controlled by a set of controller genes that regulate the SCCs. This controller genes can regulate one, two or three SCCs simultaneously. Hence, the decision-making is emanating from the SCCs who then turn on and off the fibers

Circuit type	E. coli	B. subtilis
Toggle-switch type	*galS-galR, uxuR-exuR, csgD-fliz*	*lexa-rocr, glnr-tnra*
Oscillator type	*rob ↦ marA, soxS ↦ fur, cspA ↦ hns, gadX ↦ hns,*	*sigk ↦ gere, siga ↦ spo0a*
Lock-on types		*sigf-sigg, siga-sigh, siga-sigd, sigd-swra*
Capable of various types	*crp-fis, gadW-gadX, fnr-arcA*	
FFF type	*ihf ↦ {fis,fliz} ↦ gadX-gadE* *ihf ↦ {fnr,fliz} ↦ gadX-gadE* *ihf ↦ {fnr,fliz} ↦ gadW-gadE* (see depiction of all circuits in SI)	

Table 3: List of gene circuits in *E. coli* and *B. subtilis*. The circuits found in *E. coli* are described in detail in Figure 8
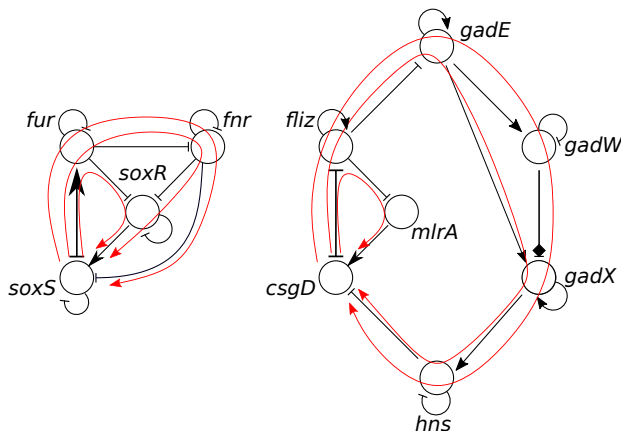

Figure 10: Example of simple directed cycles in *E. coli*. All are different cycles that cross through the logic circuits *soxS-fur* on top and *csgD-fliz* on the bottom.

under their control. So that the SCCs are crucial as the decision-making units of the TRN.

The resulting minimal network contains the strongly connected components of the network, as discussed in section **Network reduction step two: trimming the network via a k-core decomposition**, while all out-going pathways are removed by the k-core decomposition. We think that this idea may also be relevant for the design of synthetic TRNs: starting by designing the minimal core as the basic network where the minimum necessary computations are going to occur and then adding pathways outward as needed, in the form of fibers regulated by this basic minimal core.

In the case of the *E. coli* and *B. subtilis* TRNs studied, we obtained a simple structure: the SCCs of the network receiving inputs from outside controlling nodes as well as some connecting nodes between the different SCCs, responsible for transmitting signals between the SCCs. This also yields a simple and modular interpretation of the minimal TRN as the computational core driving the dynamics of the entire TRN.

Since the logical genetic circuits described in section **Small-scale structure of the core TRN: logic circuits** are contained in the SCCs, our reduction method preserves the entire computationally relevant circuitry of the original network. The controlling nodes to the SCCs act as symmetry breaking nodes giving, rise to the symmetry broken circuits, more generally acting as the inputs for the logical genetic circuits within the SCCs. We would anticipate that, unlike the carefully designed and implemented circuits in synthetic biology, the inputs external to the feedback circuit structure are crucial to the computational and biological behavior of the observed circuits and to the whole *computational apparatus* of the network, and the bacteria itself. This is why understanding the topology of the whole network and the communication between the

different modules of the network among themselves and with the extra-cellular environment becomes of great importance.

Under this perspective we can then understand the dynamics of the network in the following way: the computational core, i.e. the resulting minimal TRN, *"executes"* a response to its input signals coming from metabolism and from the extra-cellular environment; then the corresponding output is propagated through the network in a signaling cascade-like event, through the fibration tree-like structure flowing outward of the computational core to the peripheries of the network. The codes to reproduce the entire analysis in the present paper can be found in https://github.com/makselab.

3.4 Transcriptional Regulatory Network of *B. subtilis*

Next, we repeated our analysis with a second example organism, the soil bacterium *Bacillus subtilis*. *B. subtilis* is a main model organism for Gram-positive bacteria with a well-studied TRN. The data used for *B. subtilis* included not only transcriptional activators and repressors, but also sigma factors since they play a bigger role in this organism [22]. A sigma factor binds to the promoter region of a target gene to enable its transcription, and different sigma factors enable target specific groups of genes, for example, genes involved in stress responses. In our analysis, we described the action of sigma factors simply by activation edges. It has been shown before that the integrated metabolic and regulatory network of *B. subtilis* can be broken down into functional modules, locally regulated or regulated by a global regulator [22, 19]. However the overall structure of this network, how the modules interact with each other and the overall flow of information or signals between this is still not entirely understood. Same as in *E. coli*, our method allows us to understand the structure of the transcriptional regulatory network for this bacteria and as well as identifying the possible logical circuits at the core of the network. Like for *E. coli*, it was possible to classify all nodes in the TRN: in the original TRN, each node either belongs to a fiber, belongs to a logic circuit, or sends inputs to circuits.

The first fibration reduction shrinks the network size to 21% of its original size. The *k*-core reduction leads to a further reduction to just 0.9% of the original nodes, as can be seen table 4. The resulting core TRN for *B. subtilis* is shown in Fig. 12 and corresponds to just 22 nodes.

3.4.1 Large-scale structure

Like in *E. coli*, the resulting minimal set of TFs obtained for *B. subtilis* contains only the SCCs, the fibers connecting them, and the nodes sending signals to control them. It is particularly interesting, however, how this minimal gene regulatory network is smaller, with just 22 nodes in 4 SCCs, than the one for *E. coli*, given that the original network is bigger (2482 nodes). In contrast to *E. coli*, *B. subtilis*' minimal TRN is almost exclusively the SCCs with only 3 controlling nodes whereas in *E. coli* there are 18 controlling nodes that inform the SCCs modules.

The structure of the computational minimal core in *B. subtilis* is simpler than in *E. coli*. Consisting of only 4 SCCs: the *siga* SCC, a big central SCC as a hub composed of 13 nodes, which regulates the other three SCCs of only two nodes each. This hub SCC is also being controlled by two controlling nodes (*sala* and *sens*). Importantly we also find a feed-forward structure with the master regulator SCC regulating both the *sigf-sigg* and *sigk-gere* SCCs, this second SCC also receiving from *sigf-sigg*. The other SCC *lexa-rocr* only receives from the central SCC, this functions as the input to the circuit *lexa-rocr*. Two controller nodes feed directly into the central hub while the third controller node connects the *sigf-sigg* to the *sigk-gere* SCCs.

Reduction step	Gene count	%
Step 0: Full TRN	2482	100%
Step 1: Collapsing Fibers	521	21%
Step 2: Pruning	22	0.9%

Table 4: Reduction count. Full *B. subtilis* genome is 4538 genes.
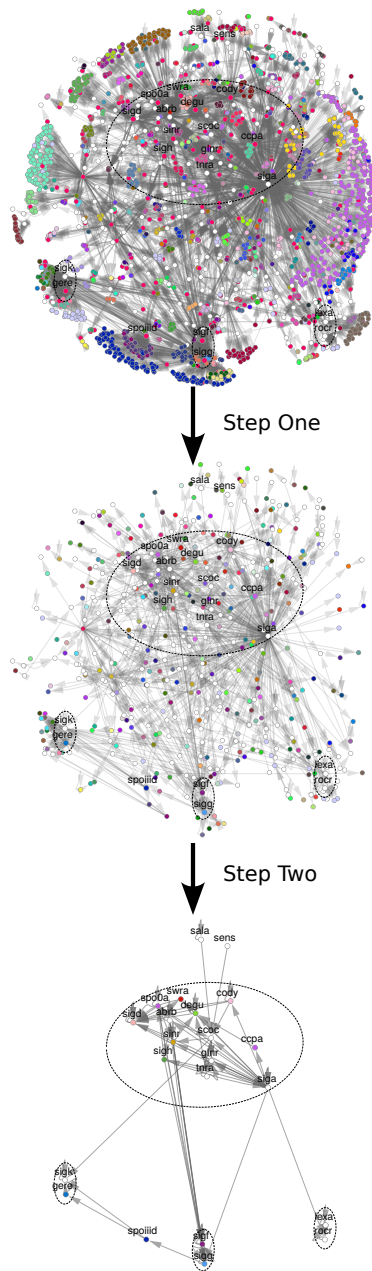
Step One

Step Two

Figure 11: Reduction steps for the *B. subtilis* TRN, as shown for *E. coli* in figure 7
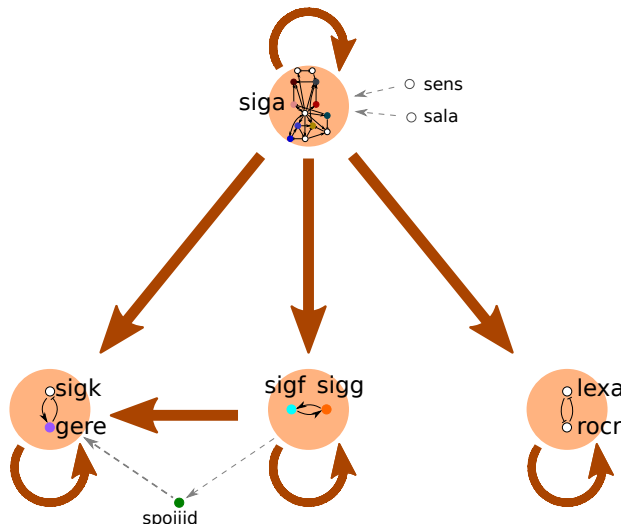
Figure 12: Reduced TRN of *B. subtilis*. The 4 SCCs are shown: *siga* SCC, *sigk-gere* SCC, *sigf-sigg* SCC, and *lexa-rocr* SCC. The signaling flows between them: with the *siga* SCC the hub controlling the other three SCC and being fed information signals by the two controllers *sens* and *sala*, controller node *spoiiid* connects the *sigk-gere* SCC and *sigf-sigg*. A feed-forward structure between the *siga* SCC and the *sigk-gere* SCC is visible.

3.4.2 Small-scale circuits

Again, we actually observe fewer logic circuits present in *B. subtilis* than in *E. coli* with only 8 in total, compared to the 12 found in *E. coli*. Of this, two correspond to MR circuits, toggle-switch types: the *lexa-rocr* SCC and *glnr-tnra* from the central SCC, as in *E. coli* both of them present additional negative auto-regulations in each gene (see SI). Two other circuits correspond to NFBL circuits (oscillating types): the *sigk ↦ gere* SCC, which actually corresponds to an amplified NFBL given that *sigk* possess a self activation and *siga ↦ spo0a* from the central SCC, actually a Smolen oscillator for its self-loops. The main difference with *E. coli* is that we observe 4 PAR feedback loop circuits, possibly *lock-on* circuits: the *sigf-sigg* SCC and the rest within the central SCC. All of them have at least one gene with an additional positive auto-regulation. In *E. coli* the only *lock-on* feedback loops present were part of the *feed-forward fiber* type circuits. See table 3 for details.

3.4.3 Cycles

We found a few more cycles in *B. subtilis* than for *E. coli*. Out of the 48 cycles, 3 correspond to the two-node SCCs and the remaining 45 cycles are located within the central SCC. As in *E. coli*, we observe that all of the cycles, except for one, cross through nodes connected by logic circuits. The exception being the cycle made by *abrb-sigh-spo0a-abrb*, although *sigh* and *spo0a* do belong to logic circuits, they don't form part of

TRN breakdown	Gene count	%
Full TRN	2482	100%
Nodes in fibers	2263	91.2%
k_{out} shell (not in fibers)	209	8.4%
Nodes in SCCs (not in fibers)	8	0.32%
Connectors (not in fibers)	2	0.08%

Table 5: Breakdown of *B. subtilis*' TRN network. Step 1 collapses the 2263 nodes in fibers into just 302 fibers, to give the Collapsed-fibers 521 node network. Step 2, removes all the Shell nodes and 290 of the fiber-collapsed nodes, this leaves only the 22 nodes present at the Minimal TRN of *B. subtilis*

31

the same circuits. There are again numerous cases in which the cycles cross through multiple nodes that are connected by a logic circuit as is shown in figure 7C for *E. coli*.

3.5 The observed network structures are statistically significant

	E. coli			B. subtilis		
	N_real	$N_\text{rand} \pm \text{SD}$	$Z - score$	N_real	$N_\text{rand} \pm \text{SD}$	$Z - score$
SCCs						
Number of SCCs	6	1.61 ± 0.74	5.93	4	1.2 ± 0.43	6.51
Average SCC size	4	10.03 ± 7.94	-0.76	4.75	25 ± 11.7	-1.73
Circuits						
Total number of circuits	13	2.02 ± 1.39	7.9	8	3.95 ± 1.98	2.05
Toggle-switch	3	0.37 ± 0.58	4.53	2	-	Inf
Toggle-switch/Osc	2	0.13 ± 0.34	5.5	0	0.6 ± 0.94	-0.64
Oscillator	5	0.7 ± 0.77	5.58	2	2.97 ± 1.86	-0.52
Lock-on	0	0.45 ± 0.64	-0.7	4	-	Inf
Lock-on/Osc	0	0.17 ± 0.38	-0.45		-	
FFF	3	0.2 ± 0.6	4.67	0	0.38 ± 0.69	-0.55
Cycles						
Number of Cycles	41	40.72 ± 70.9	0.00	48	2037.84 ± 5560	-0.36
Average Cycle Length	3.68	8.35 ± 3.53	-1.32	4.88	15.49 ± 4.43	-2.4

Table 6: Significant structures in TRNs: numbers. 100 random networks with identical in- and out-degrees of all nodes and identical edge types were generated, separately for each of *E. coli*'s and *B. subtilis*'s distributions. From these randomly generated networks we calculated the average and standard deviation quantities ($N_{rand} \pm SD$) to compare with the observed ones in the real distribution. Z-scores of each quantity were calculated to show the statistical significance of the findings.

If we find structures in graphs, we may ask whether these structures are expected in graphs of a certain type, or whether their observed numbers are unexpectedly high. In biological networks, this reflects a similar question: are the structures observed expected to appear in evolution just by chance, or are they so "unlikely" that we need to assume that they were favored by evolution for some functional benefit? To see whether the observed structures do not only emerge by chance, but are functionally relevant, we compared the *E. coli* and *B. subtilis* networks to corresponding "null hypothesis" ensembles of random graphs, following the recipe used to find significant network motifs. Our random network are supposed to represent the hypothetical outcomes of an evolution based on mutations, but without a selection for function; edges are rewired, while preserving some basic structure of the original networks (in particular, the in- and out-degrees of all individual nodes). Structures that appear in the real networks, but are rare in or absent in randomized networks can be assumed to be due to an evolutionary selection, probably for specific functional advantages. For the test, we created an ensemble of 100 random networks one corresponding to characteristics of the *E. coli* network, and another for *B. subtilis*.

To assess the statistical significance of the structures observed, we followed a standard approach: we compared our results to results from randomized networks, representing a null hypothesis. The random networks were generated through a configuration model [50], that is, a random null model that preserves the in- and out-degrees of all network nodes, along with the type of edges, while the individual connections between node pairs are randomized. In essence we rewire of the original network to randomize its edges, without adding new edges or nodes, at the end the degree (both *in* and *out*) of each node remains unchanged. This is done by repeatedly choosing two edges from the original network at random and flipping their target nodes (i.e. edges $A \mapsto B$ and $X \mapsto Y$ become $A \mapsto Y$ and $X \mapsto B$), doing so repeatedly a number of times (10000 in our case). Self-edges are not included in the flipping. We then perform the same analysis on these
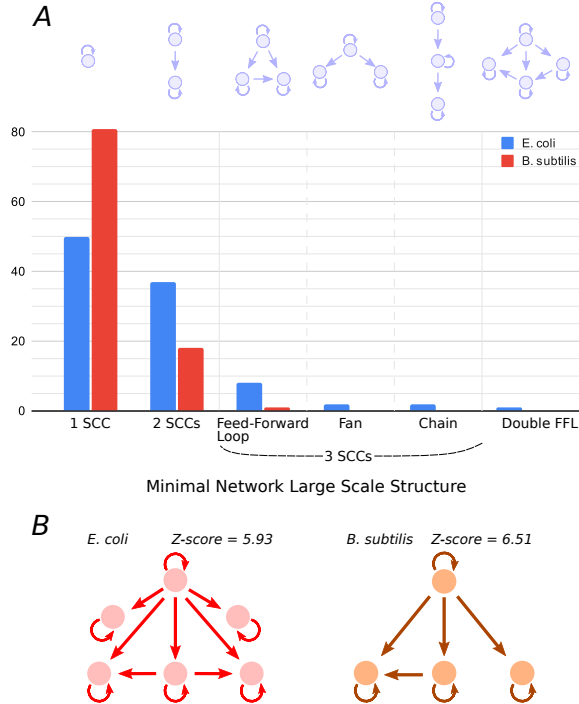
Figure 13: Significant large-scale structure in *E. coli* and *B. subtilis* core TRNs. The structure between SCCs is compared to the corresponding structure in randomized networks with the same in- and out-degrees of all nodes (and preserving the edge types). **A** Histogram illustrating the distribution of the observed structures in the core of the random networks along with a sketch of the structure itself atop the histogram. Following the format of figure 1, blue circles represent SCCs and arrows stand for edges between a node (or nodes) of one SCC to a node (or nodes) in another SCC. All observed 3 SCCs structures are shown in the darker middle section of the histogram, along with the only 4 SCCs structures found. **B** Structures observed in *E. coli*'s and *B. subtilis*'s core shown with the *Z-scores* of obtaining a structure with such number of SCCs from the randomized networks.

random networks to compare the average structures across both ensembles to what was found on *E. coli*'s and *B. subtilis*'s networks respectively. The significance of a given property (e.g the number of appearances of a specific structure) is measured by its *Z*-score from the mean values obtained from each ensemble, see table 6 for the full breakdown.

Almost all the studied structures found in both bacteria are statistically significant, as shown by their *Z*-score on table 6. All fiber classes are significantly over-abundant in the real networks, with the exception of the simplest fiber building block of only one regulator, $|n = 0, \ell = 1\rangle$, which is significantly absent. This suggests that evolved TRNs favor more complex wiring patterns, more complex fiber building blocks than just trivial ones, that allow for richer dynamics and more flexible control.

Our analysis also reveals rich structures in the core of both bacteria's networks. Not only is the number of SCCs significant (with a *Z*-score > 5 for both bacterial networks), but also the connections between the SCCs form an interesting structure for both bacteria. We can see this structure for *E. coli* in Fig. 7 and for *B. subtilis* in Figs. 12, along with simplified sketches in Figs. 13B and 1. In both networks one *"central"* SCC regulates all the other SCCs in a *feed-forward* structure (see results sections 3.3.1 and 3.4). We see two of these feed-forward structures in *E. coli* and one in *B. subtilis*, all involving the *central* SCC as the source. Most of the randomized networks, for both types of bacteria, have only one or two SCCs in their core, that is, basically no structure at all (see Fig. 13). Only 12 of the randomized *E. coli* networks show more than 2 SCCs, and only one of them shows 4 SCCs, while the ensemble of randomized *B. subtilis* networks contains only one network with 3 SCCs.

The average SCC size is not highly significant (according to its *Z*-score alone). We observe that the *size*

of the SCCs decreases as the *number* of components increases, meaning the more components were found on these random networks the smaller they were. For both *E. coli*'s and *B. subtilis'* TRNs however, we found as many as 6 and 4 SCCs, some with sizes of 11 and 13 nodes, respectively. This is in sharp contrast with any structure observed in the randomized networks. For *E. coli*, the average SCC size, if *only one* component is present, is 16.76 however, if there is *more than one* SCC, the average size now becomes 6.79; the biggest component has a size of 31 nodes for random networks with it being the only one for that particular network, on the other hand for the random networks with three components its only 18 nodes in size. The same trend is true for *B. subtilis*.

Aside from this large-scale structure, we also found a variety of logical circuits on the smaller scale, with 12 circuits in total (Z-score = 7.9) for *E. coli* and 8 circuits (Z-score = 2.05) for *B. subtilis*. The appearance of circuits is very specific. In the case of *E. coli*, the randomized networks show no preference towards any particular type of circuit: the expected count numbers for all types of circuits are lower than 1. In the real network the count numbers of the observed circuit types were much higher, with significant Z-scores, see table 6. In the *B. subtilis* random networks, there is a bias towards the presence of oscillators of which we found 2 in the real network. We also found 2 toggle-switches and 4 lock-ons, although none of the two were found in the randomized networks.

Our analysis suggests that the two bacterial networks resulted from an evolutionary selection for specific functional structures. This concerns both the large-scale substructuring of the core into several SCCs and the variety of small-scale circuits, which is far richer than that to be expected with only random mutations at play.

4 Discussion

In physics, symmetry concepts are of immense use to systematically reduce complex systems to a simpler and more transparent form while preserving the relevant characteristics of interest. As we have shown previously [52], they can also be crucial in understanding signal processing in diverse types of biological networks. Here we used fibrations to reduce gene regulatory networks, compiled from experimental data (see Section *Data and Codes*), to a minimal subnetwork that drives the dynamics of the entire network. We interpret this subnetwork as the *core computational apparatus* of the network, composed of an ensemble of logical genetic circuits.

To obtain this structure, we developed a way to systematically reduce any signal processing network to its core network responsible of driving its dynamics. In our procedure, we collapse genes which – as far as network structure alone is concerned – receive the same input signals and are therefore symmetric. In this way, we omit nodes while preserving all essential paths where signals can be transmitted. Next, we remove loose ends in the network, retaining only a core network in which signals can cycle. This core shows a simple modular structure of "signal vortices" connected in a feed-forward-manner, containing various logical circuits on the smaller scale. These logic circuits perform the computations that drive the dynamics and then through the fibrations propagate the signals to the rest of the network. Computations occur at this core network structure where the circuits are embedded in the "signal vortices", and then from there propagate to the peripheries of the network via the fiber building blocks. In this manner the information flows outwards of the core network and into the periphery of the TRN.

Our study into the TRNs of the model bacteria *E. coli* and *B. subtilis*, after network reduction, highlight the structures that control their dynamics, and show how signals can propagate in the network. "Calculations" occur only in a subset of nodes, while the others, towards the periphery of the network, just aggregate and modulate output signals. On a large scale, the core network consists of a number of vortices in which information can cycle and which are connected by feed-forward arrows. On the small scale, we found logical circuits which again may have either a feed-forward shape, transmitting signals only in one direction, or contain feed-backs (allowing for permanent inner states). While any network can be viewed in this way, we found that random networks tend to consist of one giant vortex; the actual structuring of bacterial networks into separate vortices seems to be a result of evolution and is probably functionally meaningful.

Previous work on bacterial TRNs had either been focused on local motifs and larger modules arising from their integration (i.e. FFL and Dense Overlapping Regulons) or on the coregulation of functionally related genes, thus ignoring the arrangement of genes in the overall network structure. In contrast, our

analysis considers the entire network and identifies the most influential circuits based on their placement at the core of the network. Our fibers account for global signal flows in the entire network, reaching a node under study, and allowing us to compare nodes by the global signals they receive, while the core network we find corresponds to the minimal set of nodes driving the rest of the network, the logical circuits we found embedded in the core are significant due to their influential position at the core of the network. We also recognize the importance of feedback loops in this network, a key feature that has mostly been missing from previous analysis. Feedback loops is what defines the logical circuits and the modules in our breakdown, proving to be a crucial concept.

Our approach follows a strict mathematical method to decompose the genetic network into its building blocks by using fibration symmetries and broken symmetries.

Fibrations are defined by the lifting property, which, in the context of gene regulation is akin to gene duplication and how it affects gene regulation (i.e. the edges in the TRN). This similarity may explain the existence and origin of the symmetries observed in the networks and hints that the existence of fibration symmetries on these networks may actually be a major property.

As it has been proposed for the emergence of network motifs [49, 59, 44], fibers could emerge in an evolutionary setting of random rewiring (mutation) and selection for functional structures, however, such an evolution would probably be slow. On the other hand gene duplication, may generate fiber structures fast and "for free", with subsequent minor modifications of the duplicated arrows (mutations in the regulatory region modifying incoming edges, or in the coding region modifying outgoing edges).

Let us look at this in more detail. In evolution, multiple paralogue copies of a gene may emerge via gene duplication events, and subsequent evolution may lead to differences in their coding or regulatory regions. If the gene codes for a transcription factor, the duplication will correspond to a duplication of a node in the TRN, and the subsequent changes may cause a subsequent rewiring of outgoing or incoming edges, respectively. The first step, the process of taking a gene and 'opening it up' into one or multiple other identical genes, is akin to the lifting property between a collapsed base graph and its original graph. The lifting property can be understood as 'opening up' a collapsed fiber node in the base into the full set of original synchronous nodes that share the same color. The key feature about the lifting property is that the nodes obtained by this 'opening up' have the exact same inputs and input tree as the node that is being 'opened up'. This ensures that the new network's dynamics is the same as the original collapsed base graph.

In this way, gene duplication could work as a driver for fibration symmetries in transcription regulatory networks. By duplicating a gene, in such a way that the paralogue genes share the same input relations, creates a fiber since the duplicated genes would have an isomorphic input tree. In this instance gene duplication works exactly as a lifting property, starting from the initial network and going into a new one with more symmetries and bigger fibers. Further mutations in the coding region then cause the two original copies of the gene to perform different functions, and thus diversify the bacteria's functions while creating bigger fibers.

However, if the symmetry of some of the symmetric building blocks obtained by duplication is broken, logical circuits are obtained, see section **Broken symmetry circuits: hierarchy and identification**. By taking the basic fiber building blocks in figure 2 and duplicating their bases we obtain different replica circuits still preserving the same dynamics and synchronicity. Nevertheless, if there are added regulations that break the symmetries the result is a circuit that performs logical functions, symmetry broken circuits.

Its important to point out however that you can have a duplication process that doesn't preserve the inputs. For example, a gene with a self-regulation, once duplicated would still have the self-regulation but would also now have the cross-regulation with its gene copy, meaning it went from having one input to two and changing the original input tree. Therefore, evolution or some other mechanism, is needed to ensure at least some duplication events preserve the input tree of the original gene. Perhaps evolution is selecting for duplications that preserve the dynamics of the network, hence making duplications act like liftings.

We hope that the ideas presented here can serve as inspiration to design artificial TRNs with living cell functionalities. One could start with the design of the core computational apparatus of the TRN integrating the desired amount of logical genetic circuits and then from this core network 'construct' the information highways to the peripheral genes whose products perform the required biological function. In the same vein, we think that this may also facilitate the design of minimal genomes [29].

Where are the limitations of our network reduction? First, bacterial signal processing does not depend on network structure alone, but on gene regulatory input functions with parameters that differ between genes. Even in a simple threshold model, two genes that receive inputs from the same transcription factors can

show different outputs because of different logical operations (e.g. AND versus OR) or of different activation or repression thresholds (whereby one gene is activated much more easily than the other one). Following [40], our fibration analysis ignores this complexity: it assumes that all genes in a fiber share exactly the same regulation; differences in gene regulatory functions, post-translational regulation, as well as mRNA and protein degradation are not taken into account.

But how can we justify this? In the spirit of physics, a symmetrized system can be seen as a first-order approximation, revealing some important general features of gene regulation. In this view, by considering individual gene properties we would introduce a weak symmetry breaking or second-order approximation, which changes the predicted behaviour and makes it more realistic. While the second step is important to approach biological reality, doing the first step first may provide important insights, while fully detailed, dynamic models of TRNs would prevent us from seeing the forest for the trees. Moreover, the successful implementation of genetic circuits in synthetic biology, capable of basic logical computations [20] like memory storage and time-keeping by oscillations, suggests that thinking in terms of logical circuits may also help us understand decision making in wild-type cells.

A second limitation comes from the fact that TRNs are closely linked to the rest of the cell. To trace cellular signaling flows and decision processes, a fibration analysis should not only comprise transcriptional regulation, but also metabolism. In our present analysis, metabolites may modulate of TF activity and are given inputs to the TRN. In reality, metabolite concentrations depend on enzyme activities, which themselves depend on the TRN, thus metabolic and regulatory networks form a large feedback loop. In a fibration analysis of the entire cell, these networks need to be combined. Despite some progress in this direction [24], some challenges remain. Since metabolic reactions can have multiple substrates and products, metabolic networks need to be treated as hypergraphs [4, 34]. Fibrations of hypergraphs still need to be developed. Another challenge concerns the different time scales. Metabolic dynamics is much faster than gene expression dynamics, so on the time scale of gene regulation, metabolism is close to a steady state. In this quasi-steady state, metabolite levels effectively depend on enzyme activities via long-range, non-sparse interactions [2], which complicates a fibration analysis.

To conclude, signaling in TRNs is known to be decentralized: while some "mighty" master regulators exist, there is no central agent ultimately coordinating the expression levels of all genes. However, we identified here a computational core of the network, consisting of a number of "vortices" where information can cycle and which are connected between each other in a feed-forward fashion. While any network can be dissected into such structures, the numbers and sizes of vortices we found in the TRNs are highly significant. On the smaller scale, the core contains various logical circuits. In the real network, there are additional parts that just receive signals from the core, modify their shape, and relay them to output nodes. In addition, some of the core nodes are not realized by single genes, but by fibers, that is, groups sets of genes that share the same input trees and can be expected to show similar dynamic behavior.

The outward pathways eliminated by the *'pruning'* step may come back to regulate the TRN through metabolites that control gene expression through allosteric interactions between metabolites and proteins, either, transcription factors or enzymes, alternating the activity of the protein by the binding of the effector molecule. These metabolites can *turn on and off* the edges in the TRN. Phosphorylation is another regulation of signaling processes that acts by binding a phosphate group to activate or inactivate an enzyme. These regulation processes contribute to the systems approach and integrate all regulatory process from TRN to metabolism and signaling into a TRN. While they are not considered here, they will be treated in a follow up paper.

All these (statistically significant) structures are clearly shown by our method and would not be visible otherwise: once the network was simplified by our graph fibration, the SCCs emerged by themselves, and the network structure looks suddenly simple and comprehensible! This may be a lesson for understanding other, maybe even less structured and more dynamic networks modeling other forms of collective intelligence.

5 Acknowledgments

6 Data and code availability

Network of *E.coli* obtained from RegulonDB [68] Network of *B. subtilis* obtained from SubtiWiki [56] Codes are available at: https://github.com/makselab

Declaration of conflicting interests

The author(s) declared no potential conflicts of interest with respect to the research, authorship, and/or publication of this article.

Funding

ORCID iD

Wolfram Liebermeister https://orcid.org/0000-0002-2568-2381

7 Bibliography

References

[1] Uri Alon. *An introduction to systems biology: design principles of biological circuits.* CRC press, 2019.

[2] Valentina Baldazzi, Delphine Ropers, Johannes Geiselmann, Daniel Kahn, and Hidde de Jong. Importance of metabolic coupling for the dynamics of gene expression following a diauxic shift in Escherichia coli. *Journal of Theoretical Biology*, 295:100–115, 2012.

[3] Jørgen Bang-Jensen and Gregory Z Gutin. *Digraphs: theory, algorithms and applications.* Springer Science & Business Media, 2008.

[4] Federico Battiston, Giulia Cencetti, Iacopo Iacopini, Vito Latora, Maxime Lucas, Alice Patania, Jean-Gabriel Young, and Giovanni Petri. Networks beyond pairwise interactions: structure and dynamics. *Physics Reports*, 2020.

[5] Claude Berge. *The theory of graphs.* Courier Corporation, 2001.

[6] Gordon J Berman, Daniel M Choi, William Bialek, and Joshua W Shaevitz. Mapping the stereotyped behaviour of freely moving fruit flies. *Journal of The Royal Society Interface*, 11(99):20140672, 2014.

[7] William Bialek, Andrea Cavagna, Irene Giardina, Thierry Mora, Edmondo Silvestri, Massimiliano Viale, and Aleksandra M Walczak. Statistical mechanics for natural flocks of birds. *Proceedings of the National Academy of Sciences*, 109(13):4786–4791, 2012.

[8] L. Bintu, N.E. Buchler, H.G. Garcia, U. Gerland, T. Hwa, J. Kondev, and R. Phillips. Transcriptional regulation by numbers: models. *Curr Opin Genet Dev*, 15:116–124, 2005.

[9] Paolo Boldi and Sebastiano Vigna. Fibrations of graphs. *Discrete Mathematics*, 243(1-3):21–66, 2002.

[10] Alexandre Bovet, Flaviano Morone, and Hernán A Makse. Validation of twitter opinion trends with national polling aggregates: Hillary clinton vs donald trump. *Scientific reports*, 8(1):1–16, 2018.

[11] Michael M Bronstein, Joan Bruna, Taco Cohen, and Petar Veličković. Geometric deep learning: Grids, groups, graphs, geodesics, and gauges. *arXiv preprint arXiv:2104.13478*, 2021.

[12] D Ewen Cameron, Caleb J Bashor, and James J Collins. A brief history of synthetic biology. *Nature Reviews Microbiology*, 12(5):381–390, 2014.

[13] Andrea Cavagna, Alessio Cimarelli, Irene Giardina, Giorgio Parisi, Raffaele Santagati, Fabio Stefanini, and Massimiliano Viale. Scale-free correlations in starling flocks. *Proceedings of the National Academy of Sciences*, 107(26):11865–11870, 2010.

[14] Neil Dalchau, Gregory Szép, Rosa Hernansaiz-Ballesteros, Chris P Barnes, Luca Cardelli, Andrew Phillips, and Attila Csikász-Nagy. Computing with biological switches and clocks. *Natural computing*, 17(4):761–779, 2018.

[15] Lee DeVille and Eugene Lerman. Modular dynamical systems on networks. *arXiv preprint arXiv:1303.3907*, 2013.

[16] Radu Dobrin, Qasim K Beg, Albert-László Barabási, and Zoltán N Oltvai. Aggregation of topological motifs in the {Escherichia} coli transcriptional regulatory network. *BMC bioinformatics*, 5(1):1–8, 2004.

[17] Sergey N Dorogovtsev, José Fernando F Mendes, and Alexander N Samukhin. Giant strongly connected component of directed networks. *Physical Review E*, 64(2):025101, 2001.

[18] Michael B Elowitz and Stanislas Leibler. A synthetic oscillatory network of transcriptional regulators. *Nature*, 403(6767):335–338, 2000.

[19] José P. Faria, Ross Overbeek, Ronald C. Taylor, Neal Conrad, Veronika Vonstein, Anne Goelzer, Vincent Fromion, Miguel Rocha, and Isabel Rocha Christopher S. Henry. Reconstruction of the regulatory network for Bacillus subtilis and reconciliation with gene expression data. *Front Microbiol*, 7:275, 2016.

[20] Timothy S Gardner, Charles R Cantor, and James J Collins. Construction of a genetic toggle switch in {Escherichia} coli. *Nature*, 403(6767):339–342, 2000.

[21] Naama Geva-Zatorsky, Erez Dekel, Eric Batchelor, Galit Lahav, and Uri Alon. Fourier analysis and systems identification of the p53 feedback loop. *Proceedings of the National Academy of Sciences*, 107(30):13550–13555, 2010.

[22] A. Goelzer, F. Bekkal Brikci, I. Martin-Verstraete, P. Noirot, P. Bessieres, S. Aymerich, et al. Reconstruction and analysis of the genetic and metabolic regulatory networks of the central metabolism of Bacillus subtilis. *BMC Syst. Biol.*, 2(30), 2008.

[23] Martin Golubitsky and Ian Stewart. Nonlinear dynamics of networks: the groupoid formalism. *Bulletin of the american mathematical society*, 43(3):305–364, 2006.

[24] Anne Grimbs, David F Klosik, Stefan Bornholdt, and Marc-Thorsten Hütt. A system-wide network reconstruction of gene regulation and metabolism in {Escherichia} coli. *PLoS computational biology*, 15(5):e1006962, 2019.

[25] Alexander Grothendieck. Technique de descente et théorèmes d'existence en géométrie algébrique. i. généralités. descente par morphismes fidèlement plats. *Séminaire Bourbaki*, 5:299–327, 1959.

[26] Hermann Gruber. Digraph complexity measures and applications in formal language theory. *Discrete Mathematics & Theoretical Computer Science*, 14, 2012.

[27] Frank Harary. *Graph theory*. Addison-Wesley, 1993.

[28] ABM Hasan, Hiroyuki Kurata, and Sebastian Pechmann. Improvement of the memory function of a mutual repression network in a stochastic environment by negative autoregulation. *BMC bioinformatics*, 20(1):1–14, 2019.

[29] Clyde A Hutchison, Ray-Yuan Chuang, Vladimir N Noskov, Nacyra Assad-Garcia, Thomas J Deerinck, Mark H Ellisman, John Gill, Krishna Kannan, Bogumil J Karas, Li Ma, et al. Design and synthesis of a minimal bacterial genome. *Science*, 351(6280), 2016.

[30] Donald B Johnson. Efficient algorithms for shortest paths in sparse networks. *Journal of the ACM (JACM)*, 24(1):1–13, 1977.

[31] S. Kaplan, A. Bren, A. Zaslaver, E. Dekel, and U. Alon. Diverse two-dimensional input functions control bacterial sugar genes. *Molecular Cell*, 29:786–792, 2008.

[32] Ahmad S Khalil and James J Collins. Synthetic biology: applications come of age. *Nature Reviews Genetics*, 11(5):367–379, 2010.

[33] Maksim Kitsak, Lazaros K Gallos, Shlomo Havlin, Fredrik Liljeros, Lev Muchnik, H Eugene Stanley, and Hernán A Makse. Identification of influential spreaders in complex networks. *Nature physics*, 6(11):888–893, 2010.

[34] Steffen Klamt, Utz-Uwe Haus, and Fabian Theis. Hypergraphs and cellular networks. *PLoS Comput Biol*, 5(5):e1000385, 2009.

[35] Felix Klein. *Vergleichende Betrachtungen über neuere geometrische Forschungen: Programm zum Eintritt in die philosophische Facultät und den Senat der k. Friedrich-Alexanders-Universität zu Erlangen*. Deichert, 1872.

[36] Edda Klipp, Wolfram Liebermeister, Christoph Wierling, and Axel Kowald. *Systems biology: a textbook*. John Wiley & Sons, 2016.

[37] Galit Lahav, Nitzan Rosenfeld, Alex Sigal, Naama Geva-Zatorsky, Arnold J Levine, Michael B Elowitz, and Uri Alon. Dynamics of the p53-mdm2 feedback loop in individual cells. *Nature genetics*, 36(2):147–150, 2004.

[38] Lev Davidovich Landau and Evgenii Mikhailovich Lifshitz. *Statistical Physics: Volume 5*, volume 5. Elsevier, 2013.

[39] Ian Leifer, Flaviano Morone, Saulo DS Reis, José S Andrade Jr, Mariano Sigman, and Hernán A Makse. Circuits with broken fibration symmetries perform core logic computations in biological networks. *PLoS computational biology*, 16(6):e1007776, 2020.

[40] Ian Leifer, Mishael Sánchez-Pérez, Cecilia Ishida, and Hernán A Makse. Predicting synchronized gene coexpression patterns from fibration symmetries in gene regulatory networks in bacteria. *BMC bioinformatics*, 22(1):1–34, 2021.

[41] Miriam Leon, Mae L Woods, Alex JH Fedorec, and Chris P Barnes. A computational method for the investigation of multistable systems and its application to genetic switches. *BMC systems biology*, 10(1):1–12, 2016.

[42] Hong-Wu Ma, Jan Buer, and An-Ping Zeng. Hierarchical structure and modules in the {Escherichia} coli transcriptional regulatory network revealed by a new top-down approach. *BMC bioinformatics*, 5(1):1–10, 2004.

[43] Fragkiskos D Malliaros, Christos Giatsidis, Apostolos N Papadopoulos, and Michalis Vazirgiannis. The core decomposition of networks: Theory, algorithms and applications. *The VLDB Journal*, 29(1):61–92, 2020.

[44] Shmoolik Mangan and Uri Alon. Structure and function of the feed-forward loop network motif. *Proceedings of the National Academy of Sciences*, 100(21):11980–11985, 2003.

[45] Agustino Martínez-Antonio, Sarath Chandra Janga, and Denis Thieffry. Functional organisation of {Escherichia} coli transcriptional regulatory network. *Journal of molecular biology*, 381(1):238–247, 2008.

[46] A.E. Mayo, Y. Setty, S. Shavit, A. Zaslaver, and U. Alon. Plasticity of the cis-regulatory input function of a gene. *PLoS Biol.*, 4(4):e45, 2006.

[47] Leenoy Meshulam, Jeffrey L Gauthier, Carlos D Brody, David W Tank, and William Bialek. Coarse–graining and hints of scaling in a population of 1000+ neurons. *arXiv preprint arXiv:1812.11904*, 2018.

[48] Leenoy Meshulam, Jeffrey L Gauthier, Carlos D Brody, David W Tank, and William Bialek. Coarse graining, fixed points, and scaling in a large population of neurons. *Physical review letters*, 123(17):178103, 2019.

[49] Ron Milo, Shai Shen-Orr, Shalev Itzkovitz, Nadav Kashtan, Dmitri Chklovskii, and Uri Alon. Network motifs: simple building blocks of complex networks. *Science*, 298(5594):824–827, 2002.

[50] Michael Molloy and Bruce Reed. A critical point for random graphs with a given degree sequence. *Random structures & algorithms*, 6(2-3):161–180, 1995.

[51] Higor S. Monteiro, Ian Leifer, Saulo DS Reis, José S Andrade Jr, and Hernán A. Makse. Fast algorithm to identify cluster synchrony through fibration symmetries in large information-processing networks. *Chaos*, 2021. Under review.

[52] Flaviano Morone, Ian Leifer, and Hernán A Makse. Fibration symmetries uncover the building blocks of biological networks. *Proceedings of the National Academy of Sciences*, 117(15):8306–8314, 2020.

[53] Flaviano Morone and Hernán A Makse. Symmetry group factorization reveals the structure-function relation in the neural connectome of caenorhabditis elegans. *Nature communications*, 10(1):1–13, 2019.

[54] James R Munkres. *Elements of algebraic topology*. CRC press, 2018.

[55] Kevin Oishi and Eric Klavins. Framework for engineering finite state machines in gene regulatory networks. *ACS synthetic biology*, 3(9):652–665, 2014.

[56] Tiago Pedreira, Christoph Elfmann, and Jörg Stülke. The current state of subti wiki, the database for the model organism bacillus subtilis. *Nucleic Acids Research*, 50(D1):D875–D882, 2022.

[57] Oliver Purcell, Nigel J Savery, Claire S Grierson, and Mario Di Bernardo. A comparative analysis of synthetic genetic oscillators. *Journal of The Royal Society Interface*, 7(52):1503–1524, 2010.

[58] Y. Setty, A. E. Mayo, M. G. Surette, and U. Alon. Detailed map of a cis-regulatory input function. *PNAS*, 100(13):7702–7707, 2003.

[59] Shai S Shen-Orr, Ron Milo, Shmoolik Mangan, and Uri Alon. Network motifs in the transcriptional regulation network of {Escherichia} coli. *Nature genetics*, 31(1):64–68, 2002.

[60] Greg J Stephens, Bethany Johnson-Kerner, William Bialek, and William S Ryu. Dimensionality and dynamics in the behavior of c. elegans. *PLoS computational biology*, 4(4):e1000028, 2008.

[61] Greg J Stephens, Bethany Johnson-Kerner, William Bialek, and William S Ryu. From modes to movement in the behavior of caenorhabditis elegans. *PLoS one*, 5(11):e13914, 2010.

[62] Greg J Stephens, Leslie C Osborne, and William Bialek. Searching for simplicity in the analysis of neurons and behavior. *Proceedings of the National Academy of Sciences*, 108(Supplement 3):15565–15571, 2011.

[63] I Stewart, S. D. S. Reis, M Golubitsky, and H. A. Makse. Gene regulatory circuits as biological building blocks i: Dynamics and bifurcations. *in preparation*, 2023.

[64] Ian Stewart, Martin Golubitsky, and Marcus Pivato. Symmetry groupoids and patterns of synchrony in coupled cell networks. *SIAM Journal on Applied Dynamical Systems*, 2(4):609–646, 2003.

[65] Jesse Stricker, Scott Cookson, Matthew R Bennett, William H Mather, Lev S Tsimring, and Jeff Hasty. A fast, robust and tunable synthetic gene oscillator. *Nature*, 456(7221):516–519, 2008.

[66] Andrew S Tanenbaum. *Structured computer organization.* Pearson Education India, 2016.

[67] Denis Thieffry, Araceli M Huerta, Ernesto Pérez-Rueda, and Julio Collado-Vides. From specific gene regulation to genomic networks: a global analysis of transcriptional regulation in {Escherichia} coli. *Bioessays*, 20(5):433–440, 1998.

[68] Víctor H Tierrafría, Claire Rioualen, Heladia Salgado, Paloma Lara, Socorro Gama-Castro, Patrick Lally, Laura Gómez-Romero, Pablo Peña-Loredo, Andrés G López-Almazo, Gabriel Alarcón-Carranza, et al. Regulondb 11.0: Comprehensive high-throughput datasets on transcriptional regulation in escherichia coli k-12. *Microbial Genomics*, 8(5):000833, 2022.

[69] Mark K Transtrum, Benjamin B Machta, Kevin S Brown, Bryan C Daniels, Christopher R Myers, and James P Sethna. Perspective: Sloppiness and emergent theories in physics, biology, and beyond. *The Journal of chemical physics*, 143(1):07B201_1, 2015.

[70] John J Tyson, Katherine C Chen, and Bela Novak. Sniffers, buzzers, toggles and blinkers: dynamics of regulatory and signaling pathways in the cell. *Current opinion in cell biology*, 15(2):221–231, 2003.

[71] Lav R Varshney, Beth L Chen, Eric Paniagua, David H Hall, and Dmitri B Chklovskii. Structural properties of the caenorhabditis elegans neuronal network. *PLoS computational biology*, 7(2):e1001066, 2011.